Published in final edited form as:
J Med Chem. 2012 July 12; 55(13): 6047–6060. doi:10.1021/jm300123s.

Discovery and Optimization of Benzotriazine Di-*N*-Oxides Targeting Replicating and Non-replicating *Mycobacterium tuberculosis*

Sidharth Chopra[1,3], **Gary A. Koolpe**[1], **Arlyn A. Tambo-ong**[1], **Karen N. Matsuyama**[1], **Kenneth J. Ryan**[1], **Tran B. Tran**[1], **Rupa S. Doppalapudi**[1], **Edward S. Riccio**[1], **Lalitha V. Iyer**[1], **Carol E. Green**[1], **Baojie Wan**[2], **Scott G. Franzblau**[2], and **Peter B. Madrid**[1,*]

[1]Center for Infectious Disease and Biodefense Research, Bioscience Division, SRI International, 333 Ravenswood Avenue, Menlo Park, CA 94025-3493, USA

[2]Institute for Tuberculosis Research, College of Pharmacy, University of Illinois at Chicago, 833 South Wood Street, Chicago, IL 60612-7231, USA

Abstract

Compounds bactericidal against both replicating and non-replicating Mtb may shorten the length of TB treatment regimens by eliminating infections more rapidly. Screening of a panel of antimicrobial and anticancer drug classes that are bioreduced into cytotoxic species revealed that 1,2,4-benzotriazine di-*N*-oxides (BTOs) are potently bactericidal against replicating and non-replicating Mtb. Medicinal chemistry optimization, guided by semi-empirical molecular orbital calculations, identified a new lead compound (**20q**) from this series with an MIC of 0.31 μg/mL against H37Rv and a cytotoxicity (CC_{50}) against Vero cells of 25 μg/mL. **20q** also had equivalent potency against a panel of single-drug resistant strains of Mtb and remarkably selective activity for Mtb over a panel of other pathogenic bacterial strains. **20q** was also negative in a L5178Y MOLY assay, indicating low potential for genetic toxicity. These data along with measurements of the physiochemical properties and pharmacokinetic profile demonstrate that BTOs have the potential to be developed into a new class of antitubercular drugs.

Keywords

Benzotriazine oxides; drug resistance; bioreductive drugs; antitubercular compounds; antibiotics; nonreplicating persistence; tirapazamine

Introduction

The current R&D pipeline for new tuberculosis (TB) drugs is inadequate to address emerging drug-resistant strains. Accordingly, filling the early drug development pipeline with novel therapies likely to slow additional drug resistance is urgent. Combination chemotherapy has been a standard of care for TB since the 1950s, when it was shown that combining drugs slowed the development of drug resistance, particularly for bactericidal compounds.[1] The next major breakthrough in TB treatment was the inclusion of rifampin and pyrazinamide in the multidrug cocktail because those drugs significantly accelerated the

CORRESPONDING AUTHOR INFORMATION: Peter B. Madrid, Ph.D., Associate Program Director, Center for Infectious Disease and Biodefense Research, SRI International, 333 Ravenswood Avenue, Menlo Park, California-94025, USA, Telephone: 1-650-859-2253, Fax: 1-650-859-3153, peter.madrid@sri.com.
[3]Currently at: Scientist-Fellow, Department of Biotechnology, CSIR-Central Institute for Medicinal and Aromatic Plants, P.O. CIMAP, Lucknow-226015, India.

clearance of the infection, presumably through their bactericidal activity against the populations of bacterial persisters. The currently recommended Direct Observed Therapy Short-course (DOTS) regimen, has been shown to be highly effective in treating drug-sensitive TB, but requires at least 6 months of treatment. The next major breakthrough in the treatment of TB is likely to be the development of an improved regimen that requires less treatment time, thus decreasing cost, increasing patient compliance, and slowing the emergence of multidrug-resistant TB (MDR-TB) strains.

Mycobacterium tuberculosis (Mtb) survival in stages of nonreplicating persistence (NRP) that are tolerant to many drugs provides a possible explanation for the long treatment regimens required to eliminate an infection.[2] The development of new combination therapy regimens, including drugs that are bactericidal against these NRP stages of Mtb, has the potential for shortening the length of treatment regimens. Metronidazole, a 5-nitroimidazole antibiotic primarily used for the treatment of anaerobic bacterial infections, was one of the first compounds shown to be bactericidal against NRP Mtb.[2] Two newer 5-nitroimidazoles, PA-824[3] and OPC-67683[4], have greater potencies against Mtb and are being evaluated clinically in combinations with standard TB drugs. So far, both of these 5-nitroimidazoles have been shown to have early bactericidal activity in patients.[5,6] Preclinical studies in murine models of TB indicate that including bactericidal drugs with activity against NRP Mtb in a combination regimen shortens the time required to cure mice of the infection,[7] but it remains to be determined whether these findings will translate to the ability to shorten the length of clinical treatment regimens.

To develop new drugs that shorten TB treatment, we evaluated additional classes of bioreductively-activated compounds with previously reported antimicrobial activities for their activities against Mtb H37Rv. In the current study, we identified BTOs as a new class of antitubercular compounds with many unique properties that make them well-suited for development as anti-TB drugs with the potential to shorten the length of treatment.

Results

Survey of Bioreductively-activated Antimicrobial Scaffolds

Four classes of bioreductively –activated compounds (i.e. compounds having cellular activities requiring the enzymatic transfer of electrons from reductase enzymes) were selected for screening against Mtb H37Rv. The compounds included 2- and 5-nitroimidazoles, 2-nitrofurans, quinoxaline-1,4-di-*N*-oxides, and BTOs (Figure 1). These particular classes of compounds were selected based on prior reports of known antimicrobial activities and based on availability through commercial sources or the National Cancer Institute (NCI) Developmental Therapeutics Program compound repository.[8–10] We screened the compounds for their MIC values against Mtb H37Rv strains from two sources, as well as for their MIC values against NRP Mtb in the low-oxygen recovery assay (LORA)[11] (Table 1). The primary screening was performed in two independent laboratories with different sources of the H37Rv strain to validate that the activities were not only specific for a given laboratory strain, since wide variations in lab strains of H37Rv have been reported.[12] Additionally, we tested all of the compounds for cytotoxicity against Vero cells to give a selectivity index (SI) describing the relative cytotoxicities of compounds for Mtb over a mammalian cell line.

The data from the survey of bioreductively-activated scaffolds showed that the BTOs tested had consistent activities against both actively replicating and non-replicating Mtb. The MIC values ranged from 0.57–5 μg/mL against the actively replicating H37Rv strains and from 0.37–7.3 μg/mL in the LORA model of NRP. All of the compounds had some cytotoxicity against the Vero cells with moderate SI values. Using the results of the initial survey, we

selected the anti-TB activities of the BTOs, particularly analogs of **8a**, for SAR development and optimization studies.

Synthesis and Activity of *N*-Substituted BTOs

The first set of new BTOs synthesized contained analogs with diverse substitutions at the 3-amine position of the ring. The substitutions at this position were designed to determine how steric and electronic variations at this position affected the potency and selectivity of the compounds. The side chain modified analogs were synthesized by reacting the primary amine starting materials (Figure 2) with 3-chloro-benzotriazine-1-*N*-oxide (**9**). The amine adducts were then oxidized using pertrifluoroacetic acid, prepared *in situ* by adding trifluoroacetic anhydride (TFAA) to a stirring solution of the compound in excess hydrogen peroxide. The complete oxidation took 3–4 d with additional equivalents of TFAA added until the oxidation was complete by TLC.

Results revealed that acyclic and cyclic alkyl groups of various sizes were tolerated at the 3-amine position, but that none of the modifications significantly increased the compounds' SIs. (Table 2) All of the compounds were active (MIC ≤10 μg/mL); the most active were those with very hydrophobic side chains (**8j** and **8m**). Incorporation of a polar ether group (**8i**) into the side chain resulted in a significant loss of activity, but with a comparable reduction in cytotoxicity. The overall results from this set indicated that both cyclic and acyclic substituents at this position were tolerated with the more hydrophobic groups resulting in the most potent compounds. None of the modifications in this set significantly improve the compounds' SIs, which ranged from 2.9 – 8.3.

Synthesis and Activity of Ring-substituted BTOs

The hypothesized mechanism of action for these BTOs is the bioreductive activation of the ring into a cytotoxic radical species that causes irreparable DNA damage to Mtb. Given this mechanism, the electron reduction potentials of the compounds should dictate the selectivity of the compounds for cytotoxicity to Mtb over mammalian cells. Variations to substitutions on the heterocyclic ring should significantly alter the electron reduction potentials and affect the selectivity index of the compounds.

The synthetic route for making the ring-modified BTOs began with either a substituted aniline starting material (**11**) or a substituted 2-nitroaniline (**12**) when available. (Scheme 2) The anilines were acylated, nitrated with fuming nitric acid, and then deprotected by refluxing in hydrochloric acid to give a set of 2-nitroanilines (**12**).[13] The 2-nitroanilines were then condensed with cyanamide in concentrated hydrochloric acid followed by treatment with base to form the 1,2,4-benzotriazine-(1*N*)-oxide ring. The 3-aminobenzotriazines were then converted to 3-hydroxybenzotriazines by reaction with either sodium nitrite or *tert*-butyl nitrite to form a diazonium intermediate, which was hydrolyzed with acid. The intermediates were chlorinated by refluxing in phosphorus oxychloride to make the 3-chlorobenzotriazine-(1*N*)-oxide intermediates (**14a–g**). Intermediates **14a–g** were then reacted with a subset of the primary amine side chains (Figure 2; side chains **a**, **b**, **d**, **e**, **f**, **i** and **m**). Side chains **a**, **b**, **d** and **f** were chosen because these low molecular weight side chains yielded potent compounds without adding unnecessary additional lipophilicity.[14] Side chain **i** was chosen to sample a polar group at this position and **m** was chosen because it yielded one of the most potent compounds from the series of side-chain-substituted analogs. This set of ring-substituted BTOs was then oxidized as described in Scheme 2 to give the compounds listed in Table 3.

All of the ring-substituted BTOs were tested for antitubercular activity and cytotoxicity (Table 3). The modifications to the ring substitutions resulted in a wide range of potencies

(0.15–5 μg/mL) and cytotoxicities (<2.5–100 μg/mL). Most importantly, several of the ring substitutions led to a significant increase in SI values. The general trend observed was that electron-donating substitutions led to reduced cytotoxicities against mammalian cells. That trend fits with the hypothesis that lowering the one-electron reduction potential ($E_{½}$) of the compounds may be effective in increasing SI values.15 The best compounds from this series were those with small alkyl substitutions to the benzotriazine ring, such as the 5-methyl and 6,7-cyclopentyl substitutions. These ring systems yielded compounds with SIs near 50.

Synthesis and Activity of Di-*N*-Alkyl BTOs

The SAR data from the side chain and ring-substituted compounds suggested that increasing the electron-donating groups around the benzotriazine ring increased the selectivity index and that modifying the alkylamine side chains increased potency, but did not considerably affect the SI. From these observations, we concluded it was desirable to synthesize new compounds with more electron-donating groups on the alkylamine side chain. In previous attempts, compounds with tri-substituted amine side chains could not be synthesized because the final oxidation reaction conditions did not produce the desired di-*N*-oxide product. To make these compounds, we thus explored several alternative oxidizing agents to pertrifluoroacetic acid, identifying $HOF{\cdot}CH_3CN$ as a sufficiently strong reagent to carry out the desired transformation, without producing significant overoxidation side products.[16,17] This new route allowed synthesis of a series of di-*N*-alky BTOs (Scheme 3). For this route, it proved preferable to oxidize the 3-chlorobenzotriazine intermediates so that the amine diversification step was the last step in the library synthesis from common intermediates **16** and **19**.

When tested for antitubercular activity and cytotoxicity, the new di-*N*-alkyl BTOs were found to have increased SIs (Table 4). The antitubercular activities of the compounds were generally comparable to those of the ring-substituted analogs, but cytotoxicities against Vero cells were significantly reduced. From this set of compounds, we identified several new compounds with SIs >50. From the set of secondary amine starting materials used for this set of compounds (Scheme 3), small alkyl groups were found to have the greatest activities. The addition of polar or hydrophilic groups designed to increase solubility resulted in a significant loss of anti-TB activity.

Activity Against Drug-resistant Mtb Strains

We also tested a set of the most potent and selective BTOs against a panel of single-drug resistant Mtb strains (Table 5) to determine whether or not the compounds had cross-resistance with existing TB drugs and maintained their potencies against diverse strains of Mtb. The resulting data indicated that no cross-resistance occurred and that the compounds had either equal or increased potencies against the drug-resistant strains of Mtb.

Antimicrobial Spectrum of Activity for BTOs

Given the long treatment times and complex drug combination regimens, antitubercular drugs should have a narrow spectrum of antimicrobial activity. Two BTOs, **8a** and **20q**, were profiled for their antimicrobial activities against a diverse panel of Gram-positive and Gram-negative bacterial pathogens (SI Table 1). Remarkably, the BTOs were highly selective in their activities for mycobacteria, with potent activity against Mtb and weaker activity against *M. smegmatis*. *M. abscessus*, which is naturally resistant to many classes of antibiotics, was resistant to both **8a** and **20q**.[18]

Mutagenic Potential of BTOs

A liability in developing any bioreductively-activated antimicrobial drug is the potential for mutagenicity. Because the basis for activity of these compounds is the generation of intermediate radical species, undesirable mutagenicity poses a risk, as has been documented for many classes of bioreductive drugs, including the BTO tirapazamine (TPZ).[19,20] The most convenient methodology for assessing the potential to induce genetic damage is to use the plate incorporation method with *Salmonella typhimurium* strains TA98 and TA100, commonly known as the Ames assay. The *Salmonella* tester strains have mutations in the histidine operon, a mutation that leads to defective lipopolysaccharide (*rfa*), and a deletion that covers genes involved in the synthesis of biotin (*bio*) and in the repair of ultraviolet-induced DNA damage (*uvrB*).[21,22] These mutations make the strains more permeable to many molecules and increase their susceptibility to the mutagenic effects of these molecules. Given that the hypothesized mechanism of the BTO compounds is to selectively form cytotoxic radical species in bacteria over mammalian cells, a microbial mutagenicity assay is not ideal, but was used to benchmark their activities in this assay. Two BTOs, **15fa** and **20q**, with good potency and selectivity profiles were evaluated in the Ames assay, in both the presence and absence of an Aroclor 1254-induced rat-liver metabolic activation system containing 10% S9 (MA). Individual plate counts and their means and standard deviations, along with the condition of the background lawn, are presented in SI Table 2. There were dose-related increases in the number of revertant colonies for both **15fa** and **20q** with both strains TA98 and TA100 in the presence and absence of metabolic activation. In order to assess their mutagenic potential in a non-microbial system **15fa** and **20q** were also evaluated in the mouse lymphoma cell $tk^{+/-} \rightarrow tk^{-/-}$ gene mutation (MOLY) assay—a routine genetic toxicology assay used to assess the mutagenic potential of compounds in mammalian cells (Table 6).[23,24] In the presence or absence of metabolic activation (S9), **15fa,** at non-cytotoxic dose levels of 5, 10, 25, and 50 μg/mL showed a significant increase in mutation frequency MF. For **20q**, both in the presence or absence of S9, mutation frequency did not increase at non-cytotoxic dose levels up to 100 μg/mL for 4-hr exposure and up to 10 μg/mL for 24-hr exposure in the absence of S9. In conclusion, **20q** gave negative response for mutation frequency in the presence or absence of S9.

Physiochemical Properties and Mouse Pharmacokinetics

In order to assess the potential of BTOs to be developed into orally bioavailable therapeutics, some of the physiochemical properties and ADME properties were profiled for **8a** and **20q**. The solubility of these two compounds was measured in triplicate using the shake-flask method in a 0.9% saline solution at pH 7.4. Both **8a** and **20q** had acceptable solubilities of 1.35 mg/mL and 0.28 mg/mL, respectively.

In order to validate BTOs as a new lead series for the treatment of TB, it was also important to evaluate their systemic exposure in the mouse after oral administration. Because this series of compounds is still in the proof-of-concept stage, a single dose (100 mg/kg) of **8a** and **20q** were administered to mice in order to profile the pharmacokinetics for the BTOs (Table 7). Our targeted drug candidate profile is an orally administered therapeutic that requires a maximum of once-a-day dosing, and preferable 1 – 3 times a week dosing in order to be compatible with current first line TB drugs in a fixed dose combination tablet.[25] In order to achieve this profile, a mouse elimination half-life between 4 – 12 hours is being targeted in our development program. The elimination half-life was for each compound was shorter than our ideal target values, but the T_{max} values indicate that they are rapidly absorbed after oral administration (Figure 3). Both compounds resulted in good exposure based on C_{max} and AUC values, indicating these compounds show promise for further development as antitubercular drugs.

Discussion

Bioreductively-activated antimicrobials have proven to be effective drugs for a number of different types of infections and have also been evaluated for the treatment of cancer as hypoxic cytotoxins and radiation sensitizers. These highly oxidized compounds can be selectively reduced through the transfer of electrons from reductase enzymes. The single- or double-electron reduction produces reactive intermediate species that cause irreversible cellular damage, leading to cell death. The mechanisms of bioreductive compounds allow them to inflict bactericidal activity against Mtb under various growth conditions and metabolic states, provided the activating reductase enzyme is present. Thus, the compounds may have bactericidal activity against specific metabolic subpopulations of Mtb bacilli that are commonly found in lung granulomas and are resistant to other standard therapeutics. The primary motivation for evaluating bioreductively-activated compounds as antitubercular drugs is based on the hypothesis that bactericidal compounds active against multiple subpopulations of Mtb bacilli will shorten the length of drug treatment required to eliminate an infection.

Among the panel of bioreductively-activated antimicrobial scaffolds tested against Mtb, 5-nitroimidazoles have been thoroughly explored for their antitubercular activity;[26–30] 2-nitroimidazoles (e.g., etanidazole), on the other hand, have quite different properties relating to their electron reduction potentials and have been primarily used as tumor hypoxia imaging agents.[31] In our initial screening, the 2-nitroimidazoles did not show potent activity against actively replicating Mtb, but did demonstrate some selective activity against the hypoxia-induced non-replicating Mtb. This trend mimics the activity observed in mammalian cells that 2-nitroimidazoles are selectively reduced in hypoxic, but not in normoxic, cancer cells.

The nitrofurans have been used for more than 50 years to treat bacterial and parasitic diseases. They have also been reported to have potent antitubercular activity.[32,33] Of the three nitrofurans we tested in our screen, compound **2** was the only one identified with potent activity against both replicating and non-replicating Mtb, as well as good selectivity over a mammalian cell line. Compound **2** was originally developed as a candidate antibiotic for *Staphylococcus aureus* infections, but was not advanced to development because of genetic toxicity. Despite the interesting *in vitro* activity profile of compound **2**, its genetic toxicity made it unsuitable for development as an antitubercular drug.

The quinoxaline oxides have also been evaluated as potential antitubercular agents with potent activity against replicating and non-replicating Mtb.[34–39] Members of this class have been developed that have excellent selectivities for Mtb and demonstrated efficacy in low-dose aerosol infection models in mice.[40] The quinoxaline oxides tested in our panel of bioreductively-activated compounds were originally synthesized as part of a hypoxic cytotoxin program for cancer, and the antitubercular activity they exhibited was limited. Optimizing this class of compounds for antitubercular activity has led to the development of a new class of lead compounds with potent *in vitro* activities and clear *in vivo* efficacy.[40]

Our initial survey identified BTOs as a new class of bioreductively-activated antitubercular agents with good selectivity against Mtb. BTOs are well-studied and have been developed into antitumor agents, as exemplified by the drug TPZ.[41,42] Because hypoxic areas in solid tumors resist standard chemotherapy, bioreductive hypoxic-specific cytotoxins such as TPZ have been included in combination therapies to circumvent tumor resistance and improve the effectiveness of chemotherapy.[43,44] The treatment of a TB granuloma presents a similar challenge: many of the metabolic subpopulations of Mtb found in lung granulomas resist antitubercular drugs used in conventional treatment regimens. The development of new

antitubercular agents targeting the subpopulations of Mtb resistant to other drugs may increase the overall efficacy of treatment regimens.

TPZ's selective activity toward hypoxic cells is attributed to increased activation by cytosolic and nuclear reductases that convert the drug to radical metabolites and to reduced back-oxidation to the parent compound under hypoxic conditions.[45–48] These metabolites have been shown to directly or indirectly cause double-strand DNA breaks in hypoxic cells.[49] The antitubercular activity of BTOs differs from antitumor activity in that most of the compounds tested are equally active against both actively replicating Mtb and hypoxia-induced NRP Mtb. This finding suggests that the reductases in Mtb responsible for activating the BTOs are expressed during both of the replicating and non-replicating metabolic states and that back-oxidation to the parent compound under normoxic conditions does not significantly affect antitubercular activity. A detailed investigation into the molecular mechanism for the antitubercular activity of BTOs is under investigation.

Given knowledge about TPZ and the hypothesized mechanism of action for BTOs, multiple Mtb reductases are likely to be capable of activating the parent compounds. This aspect of their activity made it difficult to rely on analysis of SAR data for the optimization of the cellular activities of the BTOs. Instead, we focused on the physiochemical properties of the compounds, such as the electron reduction potentials, to guide the design of new compounds. On the basis of our hypothesized mechanism of action, the electron reduction potentials of the BTOs are fundamentally related to their activity. The total cellular activity of compounds depends on many factors, including the ability to bind to the reductases responsible for bioactivation and enter the bacterial cytosol. The potential involvement of multiple activating reductase enzymes makes it less likely that pharmacophore-based approaches will be useful for modeling activities and guiding optimization efforts.

For many classes of bioreductively-activated classes of compounds such as the BTOs, $E_{½}$ has been shown to be a major determinant of the potency and selectivity for bioreductive cytotoxic activity, and a linear relationship has been shown to exist between the energy of the LUMO and the $E_{½}$ value.[50] Given this relationship, we used the semi-empirical calculation of LUMO energies as part of our design strategy to identify compounds with increased selectivity for Mtb over mammalian cells. Mtb uses the F_{420} deazaflavin cofactor, which has a much lower reduction potential than the classical hydrogen carrier $NAD(P)^+$ (−380 mV vs. −320 mV).[51] The use of the lower reduction potential F_{420}-requiring reductases may provide a basis for the antimicrobial selectivity for many classes of bioreductive drugs, as has been proposed for the 5-nitroimidazole PA-824.[3,15] Analysis of the calculated LUMO energies for the BTOs revealed that compounds with higher LUMO energies were generally less toxic to the mammalian Vero cell line, whereas antitubercular activities had no correlation with LUMO energies. When the CC_{50} toxicity values were plotted against the calculated LUMO energies, only a weak correlation existed (R^2 value of 0.56), which was to be expected because the overall activity was multifactorial and not based on a single molecular property. Despite this limited correlation, the calculation of LUMO energies proved a valuable predictive tool in designing new BTO compounds with less toxicity to mammalian cells and with higher SIs. The calculations indicated that LUMO energies, as expected from introducing electron-donating groups into the aromatic ring system, generally increased.

A key lead optimization challenge for developing a bioreductively-activated antitubercular drug is achieving sufficient potency and selectivity for Mtb. The SAR indicates that hydrophobic side chains generally resulted in more potent antitubercular compounds, which was expected because compounds must pass through the hydrophobic mycobacterial cell wall to exert their activity. Increasing hydrophobicity also seemed to increase cytotoxicity to

mammalian cells, presumably through increased cell permeability. Modifications to the substitutions on the BTO ring resulted in substantial changes in the selectivity of the compounds. In general, introduction of electron-withdrawing groups such as halogens, resulted in more potent compounds against Mtb (MICs of 0.15–0.31 μg/mL), but those compounds were also more cytotoxic to Vero cells. Electron-donating substitutions on the ring tended to slightly decrease potency against Mtb (MICs of 0.31–1.2 μg/mL), but substantially decreased toxicity, leading to compounds with overall improved selectivity profiles. To balance these two opposing SAR trends we selected compounds with fused tricyclic ring systems (**15f**), which had the most balanced potency and selectivity profiles.

The development of the oxidation chemistry to produce the di-*N*-alkyl BTO compounds allowed us to make compounds with 2–4 fold increases in potency against Mtb, while either maintaining or decreasing toxicity against Vero cells. All of the compounds made in this series had very good potencies (MICs of 0.31–0.62 μg/mL), except for compounds with more hydrophilic side chains containing a morpholino (**17p**), a sulfone (**20v**), or a sulfamide (**20x**); all those compounds demonstrated significant reductions in antitubercular activities (MICs of 2.5–5 μg/mL). Overall, the SAR trends suggested that optimal compounds should have electron-rich ring systems (lower $E_{½}$ values; higher LUMO energies) with hydrophobic side chains to afford compounds with maximal potencies and selectivities.

Another major challenge for the development of a safe and effective bioreductively activating antitubercular drug is the elimination of genetic toxicity and mutagenicity. These major developmental liabilities pose mechanism-based risks for any bioreductively-activated drug. Because the MOLY assay indicated that TPZ, the most advanced clinical BTO under evaluation for its anticancer activity, is mutagenic, eliminating its mutagenic activity was essential for developing it as an antitubercular drug candidate. To mitigate that risk, we increased the selectivity of the compounds sufficiently so that they did not produce the reactive radical compounds in mammalians cells that give rise to mutagenicity. Surprisingly, both of the compounds tested in the MOLY assay (**15fa** and **20q**) had similar selectivities and cytotoxicities against Vero cells, but had dramatically different mutagenic potentials. That discrepancy demonstrates the difficulty of rational approaches for reducing genetic toxicity. Fortunately, our lead compound, **20q** had no mutagenic activity at concentrations up to 100 μg/mL.

Analysis of the physiochemical properties and mouse pharmacokinetic data for **8a** and **20q** show that the class has good drug-like properties. The solubilities of the compounds are generally very good, most likely due to the polar nature of the *N*-oxide groups on the benzotriazine rings. The initial pharmacokinetics data for the series indicates that the lead compounds are not yet optimal with respect to clearance and overall exposure, but are sufficient to warrant further medicinal chemistry optimization.

In summary, the development of bioreductively-activated anti-infective drugs is a clinically proven strategy that has only recently been applied to the development of therapeutics for TB. The success of 5-nitroimidazoles such as PA-824 in preclinical and clinical studies demonstrates that developing a safe and effective therapeutic from this mechanistic class is possible. BTOs have long been known for their anticancer activity as radiation sensitizers and hypoxic cytotoxins, but the present work demonstrates that newer members of this class can be developed with potent and selective antitubercular activity. As with any new therapeutic class, the evaluation of BTOs in *in vivo* efficacy models will provide further insight into the bactericidal activity of this class and their potential for shortening the required length of therapy.

Experimental Methods

General

All reagents and starting materials were purchased from commercial sources and used without further purification. ^{1}H NMR were recorded on a Varian Utility 300 or 400 MHz spectrometer, in deuterated chloroform ($CDCl_3$), methanol (CD_3OD), or dimethyl sulfoxide (DMSO-d_6) solvent. Chemical shifts were reported as ppm downfield from an internal TMS standard ($\delta = 0.0$ for ^{1}H NMR) or from solvent reference. Coupling constants (*J* values) were measured in hertz. Low resolution electrospray mass spectra (ES-MS) were collected on a Finnigan Liquid Chromatography Quadrupole (LCQ) Duo Liquid Chromatography Tandem Mass Spectrometer (LC-MS-MS) (Thermoquest). Crude products were purified by flash chromatography using a Biotage Isolera Flash Purification System with SiliaSep-HP high-performance flash cartridges (SiliCycle). All compounds were purified to purities >95% as assessed by HPLC and ^{1}H-NMR. The HPLC method used an Ace® reversed-phase C18 column (100 × 4.6 mm, 3 μm) running a binary gradient with water (with 0.1% TFA) and acetonitrile (with 0.1% TFA). Purity was measured using the wavelengthMAX reading from a photodiode array detector scanning from 220–600 nm on a 12 min gradient running from 0% to 100% acetonitrile/TFA at 1 mL/min on a Waters Alliance HPLC. All known compounds were referenced throughout this work and data for any new compounds is given below.

General Procedure for Amination/Oxidation. Method A

A primary amine (2.2 mmol) starting material was added to a stirring solution of **9** (200 mg, 1.1 mmol) dissolved in DCM (10 mL) with triethylamine (5.5 mmol) at room temperature. The solution was stirred for 24 – 48 hours until all of the **9** starting material was consumed as monitored by TLC (5% MeOH/DCM mobile phase). The bulky amine side chains required heating to 45 °C for complete conversion. The entire reaction was evaporated under reduced pressure to give the crude products **10a–n** which were directly subjected to oxidation conditions. The crude mono-*N*-oxides were dissolved in a mixture of THF (8 mL) and 50% H_2O_2 (4 mL), then slowly treated with TFAA (3.3 mmol) while stirring at room temperature. The oxidation was monitored by TLC and additional equivalents of TFAA (3.3 mmol) were added every 12 hours until the reactions were > 90% complete or no additional product was being formed. Upon completion of the reaction, the reaction was quenched with 10 mL of saturated sodium bicarbonate and extracted three times with 10 mL of chloroform. The combined organic layers were evaporated and purified by semi-preparative reversed-phase HPLC.

General Procedure for 3-Aminobenzotriazine 1-Oxides. Method B

In a 1L 3-neck flask with mechanical stirring and a reflux condenser was placed a 2-nitroaniline (**12a–h**, 171 mmol), cyanamide (1.37 mol, 8 eq.) and Et_2O (30 mL). The mixture was heated to 100 °C for 1 hour, then cooled to 50 – 55°C. Using an addition funnel concentrated HCl (72 mL) was added dropwise with mechanical stirring (CAUTION: Highly exothermic reaction.) Once the addition is complete and there no further gas evolution, the mixture was heated to 110°C for 3 hours. The reaction was then cooled to 50°C and a NaOH solution (7.5 M, 160 mL) was slowly added. This was then reheated to 110°C with an oil bath for 3 hours, cooled and poured into 3 L of H_2O. The resulting solid was filtered off, washed with H_2O and Et_2O, then dried under vacuum. If necessary, the product was purified by flash chromatography using silica gel with a mobile phase gradient of 0 – 10% MeOH in CH_2Cl_2.

General Procedure for 3-Chlorobenzotriazine 1-Oxides. Method C

$NaNO_2$ (1.5 g, 21 mmol) was added in small portions to a stirring solution of a 3-aminobenzotriazine 1-oxide (**13a–e**, 7 mmol) in trifluoroacetic acid (15 mL) at room temperature. After 1 hour, 50 mL of H_2O was added and the solid was filtered off and dried under vacuum. The solid was then suspended in 20 mL of $POCl_3$ and heated to reflux for 3 hours. The solution was cooled, the majority of the excess $POCl_3$ was removed by distillation and then was dissolved in CH_2Cl_2 (40 mL). This solution was then washed with H_2O and brine, and the solvent was evaporated. The crude residue was purified by flash chromatography using silica gel and a gradient of 0 – 10% EtOAc in CH_2Cl_2.

General Procedure for 3-Chlorobenzotriazine 1-Oxides. Method D

tBuONO (90%, 15 mL) and H_2SO_4 (1 mL) were slowly added to a stirring solution of a 3-aminobenzotriazine 1-oxide (**13f–g**, 9 mmol) in tBuOH (50 mL) and H_2O (5 mL). After heating to 60°C overnight the mixture added to 100 g of ice and the resulting solid was filtered off and dried under vacuum. The solid was then suspended in 20 mL of $POCl_3$ and heated to reflux for 3 hours. The solution was cooled, the majority of the excess $POCl_3$ was removed by distillation and then was dissolved in CH_2Cl_2 (40 mL). This solution was then washed with H_2O and brine, and the solvent was evaporated. The crude residue was purified by flash chromatography using silica gel and a gradient of 0 – 10% EtOAc in CH_2Cl_2.

General Procedure for HOF·CH_3CN Oxidation. Method E

(CAUTION: F_2 and HOF·CH_3CN are extremely strong oxidants and corrosive materials) 10% F_2 with nitrogen was slowly bubbled into 100 mL of CH_3CN with 10 mL of H_2O for 1 hour at −15°C. The resulting oxidant was added in one portion to a cooled (0°C) solution of the benzotriazine 1-*N*-oxide (12.6 mmol) dissolved in CH_2Cl_2 (80 mL). The mixture was stirred for 10 minutes, then quenched with saturated $NaHCO_3$ (40 mL). The biphasic mixture was then diluted with H_2O (40 mL) and extracted with $CHCl_3$ (80 mL). The organic layer was then washed with H_2O, brine and dried over $MgSO_4$. Solvent was evaporated and the product was purified by flash chromatography using silica gel and a mobile phase gradient of 0 – 10% EtOAc in CH_2Cl_2. Isolated yields were from 35 – 40% with the remainder of the mass being recovered starting material.

General Procedure for Amination of 3-Chlorobenzotriazine-1,4-Di-*N*-Oxides. Method F

To a stirring solution of the 3-chlorobenzotriazine-1,4-di-*N*-oxide (2 mmol) in dimethoxyethane (12 mL) at 0°C was added an amine (2.2 mmol) and triethylamine (2.4 mmol). The mixture was allowed to warm to room temperature and was stirred for 16 hours. After the reaction, solvent was evaporated and the crude product was purified by flash chromatography using silica gel and a mobile phase gradient of 0 – 10% MeOH in CH_2Cl_2. Typical yields were from 80 – 90%.

3-(ethylamino)benzo[e][1,2,4]triazine 1,4-dioxide (8a)—Synthesized from **9** by Method A. Red solid. ^{1}H-NMR (DMSO-d_6, 400 MHz): δ 8.28 (br-s, 1H), 8.18 (d, J = 8.4 Hz, 1H), 8.10 (d, J = 8.5 Hz, 1H), 7.90 (t, J = 7.5 Hz, 1H), 7.55 (t, J = 8.6 Hz, 1H), 3.43 (m, 2H), 1.18 (t, J = 7.0 Hz, 3H). MS (ESI+): m/z 207.0 ($(M+H)^+$).

3-(cyclopropylamino)benzo[e][1,2,4]triazine 1,4-dioxide (8b)—Synthesized from **9** by Method A. Red solid. ^{1}H-NMR (DMSO-d_6, 400 MHz): δ 8.41 (d, J = 2.4 Hz, 1H), 8.20 (dd, J = 8.8, 0.8 Hz, 1H), 8.10 (dd, J = 8.8, 0.8 Hz, 1H), 7.92 (m, 1H), 7.56 (m, 1H), 2.76 (m, 1H), 0.74 (m, 4H). MS (ESI+): m/z 219.0 ($(M+H)^+$).

3-(tert-butylamino)benzo[e][1,2,4]triazine 1,4-dioxide (8c)—Synthesized from **9** by Method A. Red solid. ^{1}H-NMR (DMSO-d_6, 400 MHz): δ 8.31 (d, J = 8.8 Hz, 1H), 8.26 (d, J = 8.8 Hz, 1H), 7.83 (t, J = 7.0 Hz, 1H), 7.45 (t, J = 7.0 Hz, 1H), 7.19 (s, 1H), 1.55 (s, 9H). MS (ESI+): *m/z* 235.0 ((M+H)$^+$).

3-(cyclobutylamino)benzo[e][1,2,4]triazine 1,4-dioxide (8d)—Synthesized from **9** by Method A. Red solid. ^{1}H-NMR (DMSO-d_6, 400 MHz): δ 8.44 (d, J = 8.0 Hz, 1H), 8.17 (dd, J = 8.8, 0.8 Hz, 1H), 8.10 (dd, J = 8.8, 0.8 Hz, 1H), 7.91 (m, 1H), 7.54 (m, 1H), 4.33 (m, 1H), 2.24 (m, 4H), 1.67 (m, 2H). MS (ESI+): *m/z* 233.0 ((M+H)+).

3-(cyclopentylamino)benzo[e][1,2,4]triazine 1,4-dioxide (8e)—Synthesized from **9** by Method A. Red solid. ^{1}H-NMR (DMSO-d_6, 400 MHz): δ 8.18 (dt, J = 8.8, 0.8 Hz, 1H), 8.10-8.06 (m, 2H), 7.92 (m, 1H), 7.54 (m, 1H), 4.18 (m, 1H), 1.92 (m, 2H), 1.70 (m, 4H), 1.56 (m, 2H). MS (ESI+): *m/z* 247.0 ((M+H)+).

3-(cyclohexylamino)benzo[e][1,2,4]triazine 1,4-dioxide (8f)—Synthesized from **9** by Method A. Red solid. ^{1}H-NMR (DMSO-d_6, 400 MHz): δ 8.16 (dd, J = 8.8, 0.8 Hz, 1H), 8.08 (dt, J = 8.8, 0.8 Hz, 1H), 7.95 (d, J = 9.2 Hz, 1H), 7.89 (m, 1H), 7.52 (m, 1H), 3.71 (m, 1H), 1.85 (m, 2H), 1.72 (m, 2H), 1.58 (m, 1H), 1.51-1.42 (m, 2H), 1.35-1.26 (m, 2H), 1.20-1.09 (m, 1H). MS (ESI+): *m/z* 261.0 ((M+H)+).

3-(cycloheptylamino)benzo[e] [1,2,4]triazine 1,4-dioxide (8g)—Synthesized from **9** by Method A. Red solid. ^{1}H-NMR (DMSO-d_6, 400 MHz): δ 8.18 (dt, J = 8.8, 0.8 Hz, 1H), 8.09 (dt, J = 8.8, 0.8 Hz, 1H), 7.96 (d, J = 8.4 Hz, 1H), 7.91 (m, 1H), 7.53 (m, 1H), 3.92 (m, 1H), 1.89 (m, 2H), 1.76-1.42 (m, 10H). MS (ESI+): *m/z* 275.0 ((M+H)+).

3-(pentan-2-ylamino)benzo[e][1,2,4]triazine 1,4-dioxide (8h)—Synthesized from **9** by Method A. Red solid. ^{1}H-NMR (DMSO-d_6, 400 MHz): δ 8.16 (dt, J = 8.8, 0.4 Hz, 1H), 8.07 (dt, J = 8.8, 0.4 Hz, 1H), 8.00 (d, J = 9.2 Hz, 1H), 7.90 (m, 1H), 7.52 (m, 1H), 3.97 (m, 1H), 1.65 (m, 1H), 1.49 (m, 1H), 1.30 (m, 2H), 1.20 (d, J = 6.4 Hz, 3H), 0.83 (t, J = 7.2 Hz, 3H). MS (ESI+): *m/z* 249.0 ((M+H)+).

3-((1-methoxybutan-2-yl)amino)benzo[e][1,2,4]triazine 1,4-dioxide (8i)—Synthesized from **9** by Method A. Red solid. ^{1}H-NMR (DMSO-d_6, 400 MHz): δ 8.18 (dt, J = 8.8, 0.8 Hz, 1H), 8.09 (dt, J = 8.8, 0.8 Hz, 1H), 7.92 (m, 2H), 7.54 (m, 1H), 3.50 (dd, J = 10, 6.4 Hz, 1H), 3.40 (dd, J = 10, 5.2 Hz, 2H), 3.23 (s, 3H), 1.62 (m, 2H), 0.87 (m, 3H). MS (ESI+): *m/z* 265.0 ((M+H)+).

3-((4-(tert-butyl)cyclohexyl)amino)benzo[e][1,2,4]triazine 1,4-dioxide (8j)—Synthesized from **9** by Method A. Red solid. ^{1}H-NMR (DMSO-d_6, 400 MHz): δ 8.17 (td, J = 8.4, 0.8 Hz, 1H), 8.08 (m, 1H), 7.97 (d, J = 9.2 Hz, 1H), 7.91 (m, 1H), 7.57-7.50 (m, 1H), 4.06 (m, 1H), 1.94 (m, 2H), 1.75 (m, 1H), 1.58 (m, 2H), 1.14 (m, 4H), 0.83 (d, J = 3.2 Hz, 9H). MS (ESI+): *m/z* 317.1 ((M+H)+).

(R)-3-((1-cyclohexylethyl)amino)benzo[e][1,2,4]triazine 1,4-dioxide (8k)—Synthesized from **9** by Method A. Red solid. ^{1}H-NMR (DMSO-d_6, 400 MHz): δ 8.16 (dd, J = 8.8, 0.8 Hz, 1H), 8.08 (dd, J = 8.8, 0.8 Hz, 1H), 7.89 (m, 2H), 7.51 (m, 1H), 3.75 (m, 1H), 1.72-1.55 (m, 6H), 1.18 (d, J = 6.8 Hz, 3H), 1.12 (m, 3H), 0.92 (m, 2H). MS (ESI+): *m/z* 289.0 ((M+H)+).

3-((5-methylhexan-2-yl)amino)benzo[e][1,2,4]triazine 1,4-dioxide (8l)—Synthesized from **9** by Method A. Red solid. ^{1}H-NMR (DMSO-d_6, 400 MHz): δ 8.16 (dd, J

= 8.8, 0.8 Hz, 1H), 8.09 (dd, *J* = 8.4, 0.4 Hz, 1H), 7.94 (d, *J* = 9.6 Hz, 1H), 7.89 (m, 1H), 7.52 (m, 1H), 3.91 (m, 1H), 1.66 (m, 1H), 1.50 (m, 2H), 1.20 (d, *J* = 6.8 Hz, 3H), 1.15 (m, 2H), 0.83 (dd, *J* = 6.4, 2.0 Hz, 6H). MS (ESI+): *m/z* 277.0 ((M+H)+).

3-((1R,2R,4S)-bicyclo[2.2.1]heptan-2-ylamino)benzo[e][1,2,4]triazine 1,4-dioxide (8m)—Synthesized from **9** by Method A. Red solid. ^{1}H-NMR (DMSO-d_6, 400 MHz): δ 8.18 (dt, *J* = 8.8, 0.4 Hz, 1H), 8.09 (dd, *J* = 8.8, 0.8 Hz, 1H), 7.90 (m, 1H), 7.73 (d, *J* = 6.8 Hz, 1H), 7.53 (m, 1H), 3.65 (m, 1H), 2.26 (m, 2H), 1.69 (m, 2H), 1.50 (m, 3H), 1.14 (m, 3H). MS (ESI+): *m/z* 273.0 ((M+H)+).

3-((1R,3S,5r,7r)-adamantan-2-ylamino)benzo[e][1,2,4]triazine 1,4-dioxide (8n)—Synthesized from **9** by Method A. Red solid. ^{1}H-NMR (DMSO-d_6, 400 MHz): δ 8.18 (dd, *J* = 8.8, 0.8 Hz, 1H), 8.11 (dd, *J* = 8.8, 1.2 Hz, 1H), 7.93 (m, 1H), 7.55 (m, 1H), 7.39 (d, *J* = 8.4 Hz, 1H), 4.00 (m, 1H), 2.04 (m, 2H), 1.88 (m, 8H), 1.72 (br s, 2H), 1.61 (m, 2H). MS (ESI+): *m/z* 313.1 ((M+H)+).

3-(ethylamino)-7-fluorobenzo[e][1,2,4]triazine 1,4-dioxide (15aa)—Synthesized from 4-fluoro-2-nitroaniline using Method C and Method A. Red solid. ^{1}H-NMR ($CDCl_3$, 400 MHz): δ 8.26 (dd, *J* = 4.9, 9.6; 1H), 7.92 (dd, *J* = 1.7, 8.0; 1H), 7.57 (m, 1H), 6.94 (br-t, 1H), 3.57 (p, *J* = 7.3, 2H), 1.29 (t, *J* = 7.3, 3H). MS (ESI+): *m/z* 224.9 ((M+H)+).

3-(cyclopropylamino)-7-fluorobenzo[e][1,2,4]triazine 1,4-dioxide (15ab)—Synthesized from 4-fluoro-2-nitroaniline using Method C and Method A. Red solid. ^{1}H-NMR (DMSO-d_6, 400 MHz): δ 8.37 (br s, 1H), 8.15 (dd, *J* = 9.6, 5.2 Hz, 1H), 7.97 (dd, *J* = 8.4, 2.8 Hz, 1H), 7.84 (m, 1H), 2.72 (m, 1H), 0.72 (m, 4H). MS (ESI+): *m/z* 236.9 ((M+H)+).

3-(cyclobutylamino)-7-fluorobenzo[e][1,2,4]triazine 1,4-dioxide (15ad)—Synthesized from 4-fluoro-2-nitroaniline using Method C and Method A. Red solid. ^{1}H-NMR (DMSO-d_6, 400 MHz): δ 8.43 (d, *J* = 8.0 Hz, 1H), 8.15 (dd, *J* = 9.6, 5.2 Hz, 1H), 7.93 (dd, *J* = 8.8, 2.8 Hz, 1H), 7.83 (m, 1H), 4.30 (m, 1H), 2.23 (m, 4H), 1.67(m, 2H). MS (ESI+): *m/z* 250.9 ((M+H)+).

3-(cyclopentylamino)-7-fluorobenzo[e][1,2,4]triazine 1,4-dioxide (15ae)—Synthesized from 4-fluoro-2-nitroaniline using Method C and Method A. Red solid. ^{1}H-NMR (DMSO-d_6, 400 MHz): δ 8.14 (dd, *J* = 9.6, 5.2 Hz, 1H), 7.97 (m, 1H), 7.94 (dd, *J* = 8.4, 2.8 Hz, 1H), 7.83 (m, 1H), 4.13 (m, 1H), 1.91 (m, 2H), 1.67(m, 4H), 1.55 (m, 2H). MS (ESI+): *m/z* 265.0 ((M+H)+).

7-fluoro-3-((1-methoxybutan-2-yl)amino)benzo[e][1,2,4]triazine 1,4-dioxide (15ag)—Synthesized from 4-fluoro-2-nitroaniline using Method C and Method A. Red solid. ^{1}H-NMR (DMSO-d_6, 400 MHz): δ 8.16 (dd, *J* = 9.6, 5.2 Hz, 1H), 7.95 (dd, *J* = 9.2, 2.8 Hz, 1H), 7.85 (m, 2H), 3.95 (m, 1H), 3.49 (dd, *J* = 10, 6.4 Hz, 1H), 3.39 (dd, *J* = 9.6, 5.2 Hz, 1H), 3.23 (s, 3H), 1.61 (m, 2H), 0.86 (t, *J* = 7.2 Hz, 3H). MS (ESI+): *m/z* 283.0 ((M+H)+).

3-(cyclohexylamino)-7-fluorobenzo[e][1,2,4]triazine 1,4-dioxide (15aj)—Synthesized from 4-fluoro-2-nitroaniline using Method C and Method A. Red solid. ^{1}H-NMR (DMSO-d_6, 400 MHz): δ 8.14 (dd, *J* = 9.2, 5.2 Hz, 1H), 7.95 (dd, *J* = 8.8, 2.8 Hz, 1H), 7.91 (m, 1H), 7.83 (m, 1H), 3.69 (m, 1H), 1.84 (m, 2H), 1.71 (m, 2H), 1.58 (m, 1H), 1.51-1.41 (m, 2H), 1.35-1.25 (m, 2H), 1.12 (m, 1H). MS (ESI+): *m/z* 279.0 ((M+H)+).

3-((1R,2R,4S)-bicyclo[2.2.1]heptan-2-ylamino)-7-fluorobenzo[e][1,2,4]triazine 1,4-dioxide (15an)—Synthesized from 4-fluoro-2-nitroaniline using Method C and Method A. Red solid. ^{1}H-NMR (DMSO-d_6, 400 MHz): δ 8.15 (dd, J = 9.6, 4.8 Hz, 1H), 7.95 (dd, J = 9.2, 2.8 Hz, 1H), 7.84 (m, 1H), 7.74 (d, J = 7.2 Hz, 1H), 3.61 (m, 1H), 2.28 (d, J = 4.0 Hz, 1H), 2.22 (br s, 1H), 1.69 (m, 2H), 1.56 (m, 1H), 1.45 (m, 2H), 1.12 (m, 3H). MS (ESI+): *m/z* 291.0 ((M+H)+).

7-chloro-3-(ethylamino)benzo[e][1,2,4]triazine 1,4-dioxide (15ba)—Synthesized from 4-chloro-2-nitroaniline using Method C and Method A. Red solid. ^{1}H-NMR (DMSO-d_6, 400 MHz): δ 8.41 (t, J = 6.0 Hz, 1H), 8.19 (d, J = 2.4 Hz, 1H), 8.10 (d, J = 9.2 Hz, 1H), 7.91 (dd, J = 9.2, 2.4 Hz, 1H), 3.41 (m, 2H), 1.17 (t, J = 7.2 Hz, 3H). MS (ESI+): *m/z* 241.0 ((M+H)+).

7-chloro-3-(cyclopropylamino)benzo[e][1,2,4]triazine 1,4-dioxide (15bb)—Synthesized from 4-chloro-2-nitroaniline using Method C and Method A. Red solid. ^{1}H-NMR (DMSO-d_6, 400 MHz): δ 8.47 (br s, 1H), 8.19 (d, J = 2.0 Hz, 1H), 8.09 (d, J = 9.2 Hz, 1H), 7.90 (dd, J = 9.2, 2.0 Hz, 1H), 2.73 (m, 1H), 0.77-0.67 (m, 4H). MS (ESI+): *m/z* 253.0 ((M+H)+).

7-chloro-3-(cyclobutylamino)benzo[e][1,2,4]triazine 1,4-dioxide (15bd)—Synthesized from 4-chloro-2-nitroaniline using Method C and Method A. Red solid. ^{1}H-NMR (DMSO-d_6, 400 MHz): δ 8.55 (d, J = 7.6 Hz, 1H), 8.16 (d, J = 1.6 Hz, 1H), 8.09 (d, J = 9.2 Hz, 1H), 7.89 (dd, J = 9.2, 2.0 Hz, 1H), 4.31 (m, 1H), 2.22 (m, 4H), 1.66 (m, 2H). MS (ESI+): *m/z* 267.0 ((M+H)+).

7-chloro-3-((1-methoxybutan-2-yl)amino)benzo[e][1,2,4]triazine 1,4-dioxide (15bg)—Synthesized from 4-chloro-2-nitroaniline using Method C and Method A. Red solid. ^{1}H-NMR (DMSO-d_6, 400 MHz): δ 8.18 (d, J = 2.4 Hz, 1H), 8.10 (d, J = 9.2 Hz, 1H), 7.96 (d, J = 8.8 Hz, 1H), 7.90 (dd, J = 9.2, 2.4 Hz, 1H), 3.97 (m, 1H), 3.49 (dd, J = 9.6, 6.4 Hz, 1H), 3.39 (m, 1H), 3.23 (m, 3H), 1.61 (m, 2H), 0.86 (t, J = 7.2 Hz, 3H). MS (ESI+): *m/z* 299.0 ((M+H)+).

7-chloro-3-(cyclohexylamino)benzo[e][1,2,4]triazine 1,4-dioxide (15bj)—Synthesized from 4-chloro-2-nitroaniline using Method C and Method A. Red solid. ^{1}H-NMR (DMSO-d_6, 400 MHz): δ 8.17 (d, J = 2.4 Hz, 1H), 8.08 (d, J = 9.2 Hz, 1H), 8.02 (d, J = 8.8 Hz, 1H), 7.89 (dd, J = 9.2, 2.4 Hz, 1H), 3.70 (m, 1H), 1.82 (m, 2H), 1.70 (m, 2H), 1.57 (m, 1H), 1.46 (m, 2H), 1.31 (m, 2H), 1.12 (m, 1H). MS (ESI+): *m/z* 295.1 ((M+H)+).

3-((1R,2R,4S)-bicyclo[2.2.1]heptan-2-ylamino)-7-chlorobenzo[e][1,2,4]triazine 1,4-dioxide (15bn)—Synthesized from 4-chloro-2-nitroaniline using Method C and Method A. Red solid. ^{1}H-NMR (DMSO-d_6, 400 MHz): δ 8.18 (dd, J = 2.4, 0.4 Hz, 1H), 8.08 (dd, J = 9.6, 0.8 Hz, 1H), 7.90 (dd, J = 9.2, 2.4 Hz, 1H), 7.85 (m, 1H), 3.62 (m, 1H), 2.28 (d, J = 4.0 Hz, 1H), 2.22 (br s, 1H), 1.69 (m, 2H), 1.56 (m, 1H), 1.47 (m, 2H), 1.14 (m, 3H). MS (ESI+): *m/z* 307.1 ((M+H)+).

7-bromo-3-(ethylamino)benzo[e][1,2,4]triazine 1,4-dioxide (15ca)—Synthesized from 4-bromo-2-nitroaniline using Method C and Method A. Red solid. ^{1}H-NMR (DMSO-d_6, 400 MHz): δ 8.41 (t, J = 6.4 Hz, 1H), 8.32 (m, 1H), 8.01 (m, 2H), 3.40 (m, 2H), 1.17 (t, J = 7.2 Hz, 3H). MS (ESI+): *m/z* 286.9 ((M+H)+).

7-bromo-3-(cyclobutylamino)benzo[e][1,2,4]triazine 1,4-dioxide (15cd)—from Synthesized from 4-bromo-2-nitroaniline using Method C and Method A. Red solid. ^{1}H-

NMR (DMSO-d_6, 400 MHz): δ 8.58 (m, 1H), 8.31 (m, 1H), 8.02 (m, 2H), 4.32 (m, 1H), 2.32 (m, 4H), 1.67 (m, 2H). MS (ESI+): *m/z* 312.9 ((M+H)+).

7-bromo-3-(cyclopentylamino)benzo[e][1,2,4]triazine 1,4-dioxide (15ce)— Synthesized from 4-bromo-2-nitroaniline using Method C and Method A. Red solid. ^{1}H-NMR (DMSO-d_6, 400 MHz): δ 8.32 (t, J = 1.2 Hz, 1H), 8.14 (d, J = 8.0 Hz, 1H), 8.01 (m, 2H), 4.16 (m, 1H), 1.92 (m, 2H), 1.70 (m, 4H), 1.56 (m, 2H). MS (ESI+): *m/z* 326.9 ((M+H)+).

3-((1R,2R,4S)-bicyclo[2.2.1]heptan-2-ylamino)-7-bromobenzo[e][1,2,4]triazine 1,4-dioxide (15cn)—Synthesized from 4-bromo-2-nitroaniline using Method C and Method A. Red solid. ^{1}H-NMR (DMSO-d_6, 400 MHz): δ 8.33 (t, J = 1.2 Hz, 1H), 8.02 (m, 2H), 7.89 (m, 1H), 3.62 (m, 1H), 2.30 (m, 1H), 2.23 (m, 1H), 1.72 (m, 2H), 1.59-1.40 (m, 3H), 1.23-1.01 (m, 3H). MS (ESI+): *m/z* 352.9 ((M+H)+).

3-(ethylamino)-7-methoxybenzo[e][1,2,4]triazine 1,4-dioxide (15da)— Synthesized from 4-methoxy-2-nitroaniline using Method C and Method A. Red solid. ^{1}H-NMR (DMSO-d_6, 400 MHz): δ 8.08 (t, J = 6.0 Hz, 1H), 8.04 (d, J = 9.6 Hz, 1H), 7.57 (dd, J = 9.6, 2.8 Hz, 1H), 7.46 (d, J = 2.4 Hz, 1H), 3.90 (s, 3H), 3.38 (m, 2H), 1.17 (t, J = 7.2 Hz, 3H). MS (ESI+): *m/z* 237.0 ((M+H)+).

3-(cyclobutylamino)-7-methoxybenzo[e][1,2,4]triazine 1,4-dioxide (15dd)— Synthesized from 4-methoxy-2-nitroaniline using Method C and Method A. Red solid. ^{1}H-NMR (DMSO-d_6, 400 MHz): δ 8.25 (d, J = 8.0 Hz, 1H), 8.05 (d, J = 9.6 Hz, 1H), 7.57 (dd, J = 9.2, 2.8 Hz, 1H), 7.45 (d, J = 2.4 Hz, 1H), 4.30 (m, 1H), 3.90 (s, 3H), 2.22 (m, 4H), 1.67 (m, 2H). MS (ESI+): *m/z* 263.0 ((M+H)+).

3-((1R,2R,4S)-bicyclo[2.2.1]heptan-2-ylamino)-7-methoxybenzo[e][1,2,4]triazine 1,4-dioxide (15dn)—Synthesized from 4-methoxy-2-nitroaniline using Method C and Method A. Red solid. ^{1}H-NMR (DMSO-d_6, 400 MHz): δ 8.04 (d, J = 9.6 Hz, 1H), 7.56 (m, 2H), 7.46 (d, J = 2.4 Hz, 1H), 3.90 (s, 3H), 3.61 (m, 1H), 2.30 (d, J = 4.0 Hz, 1H), 2.23 (br s, 1H), 1.69 (m, 2H), 1.57-1.35 (m, 3H), 1.23-1.09 (m, 3H). MS (ESI+): *m/z* 303.0 ((M+H)+).

Ethyl-(5-methyl-1,4-dioxy-benzo[1,2,4]triazin-3-yl)-amine (15ea)—Synthesized from 6-methyl-2-nitroaniline using Method C and Method A. Red solid. ^{1}H-NMR (DMSO-d_6, 400 MHz): δ 8.34 (t, J = 6.4 Hz, 1H), 8.05 (dq, J = 8.8, 0.8 Hz, 1H), 7.60 (m, 1H), 7.38 (m, 1H), 3.40 (p, J = 6.8 Hz, 2H), 2.95 (s, 3H), 1.18 (t, J = 7.2 Hz, 3H). MS (ESI+): *m/z* 221.0 ((M+H)+).

3-(cyclobutylamino)-5-methylbenzo[e][1,2,4]triazine 1,4-dioxide (15ed)— Synthesized from 6-methyl-2-nitroaniline using Method C and Method A. Red solid. ^{1}H-NMR (DMSO-d_6, 400 MHz): δ 8.43 (d, J = 8.0 Hz, 1H), 8.04 (d, J = 8.8 Hz, 1H), 7.59 (dt, J = 7.2, 1.2 Hz, 1H), 7.38 (m, 1H), 4.31 (m, 1H), 2.96 (s, 3H), 2.27-2.17 (m, 4H), 1.68 (m, 2H). MS (ESI+): *m/z* 247.0 ((M+H)+).

3-(cyclopentylamino)-5-methylbenzo[e][1,2,4]triazine 1,4-dioxide (15ee)— Synthesized from 6-methyl-2-nitroaniline using Method C and Method A. Red solid. ^{1}H-NMR (DMSO-d_6, 400 MHz): δ 8.05 (m, 1H), 7.95 (d, J = 7.6 Hz, 1H), 7.59 (dt, J = 7.2, 1.2 Hz, 1H), 7.38 (dd, J = 8.8, 7.2 Hz, 1H), 4.15 (m, 1H), 2.96 (s, 3H), 1.94 (m, 2H), 1.68 (m, 4H), 1.57 (m, 2H). MS (ESI+): *m/z* 261.0 ((M+H)+).

3-(ethylamino)-7,8-dihydro-6H-indeno[5,6-e][1,2,4]triazine 1,4-dioxide (15fa)— Synthesized from 6-nitro-2,3-dihydro-1H-inden-5-amine using Method D and Method A. Red solid. ^{1}H-NMR ($CDCl_3$, 400 MHz): δ 8.11 (s, 1H), 8.07 (s, 1H), 6.94 (br-t, 1H), 3.59 (p, J = 7.2, 2H), 3.09 (t, J = 6.7, 2H), 3.03 (t, J = 7.7, 2H), 2.20 (p, J = 7.5, 2H), 1.33 (t, J = 7.3, 3H). MS (ESI+): *m/z* 247.0 ((M+H)+).

Cyclobutyl-(5,8-dioxy-2,3-dihydro-1H-5,6,8-triaza-cyclopenta[b]naphthalen-7-yl)-amine (15fd)—Synthesized from 6-nitro-2,3-dihydro-1H-inden-5-amine using Method D and Method A. Red solid. ^{1}H-NMR (DMSO-d_6, 400 MHz): δ 8.32 (d, J = 8.0 Hz, 1H), 7.99 (br s, 1H), 7.95 (br s, 1H), 4.32 (m, 1H), 3.07-2.97 (m, 4H), 2.22 (m, 4H), 2.07 (m, 2H), 1.67 (m, 2H). MS (ESI+): *m/z* 273.0 ((M+H)+).

3-((1R,2R,4S)-bicyclo[2.2.1]heptan-2-ylamino)-7,8-dihydro-6H-indeno[5,6-e][1,2,4]triazine 1,4-dioxide (15fn)—Synthesized from 6-nitro-2,3-dihydro-1H-inden-5-amine using Method D and Method A. Red solid. ^{1}H-NMR (DMSO-d_6, 400 MHz): δ 8.00 (br s, 1H), 7.94 (br s, 1H), 7.63 (d, J = 6.8 Hz, 1H), 3.63 (m, 1H), 3.07-2.97 (m, 4H), 2.30 (d, J = 4.0 Hz, 1H), 2.24 (br s, 1H), 2.07 (m, 2H), 1.70 (m, 2H), 1.57 (m, 1H), 1.49 (m, 2H), 1.15 (m, 3H). MS (ESI+): *m/z* 313.0 ((M+H)+).

3-(ethylamino)-6-methoxy-7-methylbenzo[e][1,2,4]triazine 1,4-dioxide (15ga)— Synthesized from 5-methoxy-4-methyl-2-nitroaniline using Method D and Method A. Red solid. ^{1}H-NMR (DMSO-d_6, 400 MHz): δ 8.17 (t, J = 6.0 Hz, 1H), 7.99 (d, J = 1.2 Hz, 1H), 7.33 (s, 1H), 4.00 (s, 3H), 3.42-3.36 (m, 2H), 2.26 (d, J = 0.8 Hz, 3H), 1.17 (t, J = 7.2 Hz, 3H). MS (ESI+): *m/z* 251.0 ((M+H)+).

3-(cyclobutylamino)-6-methoxy-7-methylbenzo[e][1,2,4]triazine 1,4-dioxide (15gd)—Synthesized from 5-methoxy-4-methyl-2-nitroaniline using Method D and Method A. Red solid. ^{1}H-NMR (DMSO-d_6, 400 MHz): δ 8.31 (d, J = 8.4 Hz, 1H), 7.98 (m, 1H), 7.33 (s, 1H), 4.31 (m, 1H), 4.00 (s, 3H), 2.26 (d, J = 0.8 Hz, 3H), 2.22 (m, 4H), 1.67 (m, 2H). MS (ESI+): *m/z* 277.0 ((M+H)+).

3-((1R,2R,4S)-bicyclo[2.2.1]heptan-2-ylamino)-6-methoxy-7-methylbenzo[e][1,2,4]triazine 1,4-dioxide (15gn)—Synthesized from 5-methoxy-4-methyl-2-nitroaniline using Method D and Method A. Red solid. ^{1}H-NMR (DMSO-d_6, 400 MHz): δ 8.01 (d, J = 1.2 Hz, 1H), 7.60 (d, J = 6.8 Hz, 1H), 7.32 (s, 1H), 4.00 (s, 3H), 3.63 (m, 1H), 2.33 (m, 1H), 2.27 (s, 3H), 2.24 (br s, 1H), 1.69 (m, 2H), 1.49 (m, 3H), 1.16 (m, 3H). MS (ESI+): *m/z* 317.0 ((M+H)+).

3-chlorobenzo[e][1,2,4]triazine 1,4-dioxide (16)—Synthesized from **9** by Method E. Yellow solid. ^{1}H-NMR ($CDCl_3$, 300 MHz): δ 8.55 (d, J = 8.5, 1H), 8.48 (d, J = 8.6, 1H), 8.07 (t, J = 8.5 Hz, 1H), 7.90 (t, J = 8.6 Hz, 1H). MS (ESI+): *m/z* 198.0 ((M+H)+).

3-chloro-7,8-dihydro-6H-indeno[5,6-e][1,2,4]triazine 1,4-dioxide (19)— Synthesized from **18** by Method E. Yellow solid. ^{1}H-NMR ($CDCl_3$, 300 MHz): δ 8.34 (s, 1H), 8.26 (s, 1H), 3.17 (q, J = 7.8 Hz, 4H), 2.27 (quin, J = 7.8, 2H). MS (ESI+): *m/z* 238.0 ((M+H)+).

3-(diethylamino)benzo[e][1,2,4]triazine 1,4-dioxide (17o)—Synthesized from **16** using Method F. Red solid. ^{1}H-NMR ($CDCl_3$, 300 MHz): δ 8.36 (d, J = 7.4 Hz, 1H), 8.31 (d, J = 7.4 Hz, 1H), 7.85 (t, J = 7.4 Hz, 1H), 7.54 (t, J = 7.4 Hz, 1H), 3.81 (q, J = 6.9 Hz, 4H), 1.32 (t, J = 7.0 Hz, 6H). (ESI+): *m/z* 235.0 ((M+H)+).

3-morpholinobenzo[e][1,2,4]triazine 1,4-dioxide (17p)—Synthesized from **16** using Method F. Red solid. ^{1}H-NMR ($CDCl_3$, 300 MHz): δ 8.39 (d, J = 8.7 Hz, 1H), 8.35 (d, J = 9.6 Hz, 1H), 7.90 (t, J = 7.0 Hz, 1H), 7.65 (t, J = 7.0, 1H), 3.91 (m, 4H), 3.87 (m, 4H). (ESI +): *m/z* 249.1 ((M+H)+).

3-(pyrrolidin-1-yl)benzo[e][1,2,4]triazine 1,4-dioxide (17q)—Synthesized from ***16*** using Method F. Red solid. ^{1}H-NMR ($CDCl_3$, 300 MHz): δ 8.31 (d, J = 5.8 Hz, 2H), 7.84 (t, J = 5.8, 1H), 7.49 (t, J = 5.8 Hz, 1H), 4.04 (m, 4H), 1.98 (m, 4H). (ESI+): *m/z* 233.0 ((M+H) +).

3-(pyrrolidin-1-yl)-7,8-dihydro-6H-indeno[5,6-e][1,2,4]triazine 1,4-dioxide (20q) —Synthesized from **19** using Method F. Red solid. ^{1}H-NMR ($CDCl_3$, 300 MHz): δ 8.11 (s, 1H), 8.10 (s, 1H), 4.03 (t, J = 6.6, 4H), 3.07 (t, J = 7.3 Hz, 2H), 3.04 (t, J = 7.5 Hz, 2H), 2.19 (quin, J = 7.4 Hz, 2H), 1.98 (m, 4H). MS (ESI+): *m/z* 273.0 ((M+H)+).

3-(piperidin-1-yl)-7,8-dihydro-6H-indeno[5,6-e][1,2,4]triazine 1,4-dioxide (20r)— Synthesized from **19** using Method F. Red solid. ^{1}H-NMR ($CDCl_3$, 300 MHz): δ 8.15 (s, 1H), 8.11 (s, 1H), 3.76 (m, 4H), 3.05 (m, 4H), 2.18 (quintet, J = 7.5 Hz, 2H), 1.69 (m, 6H). MS (ESI+): *m/z* 287.0 ((M+H)+).

3-(dimethylamino)-7,8-dihydro-6H-indeno[5,6-e][1,2,4]triazine 1,4-dioxide (20s) —Synthesized from **19** using Method F. Red solid. ^{1}H-NMR ($CDCl_3$, 300 MHz): δ 8.15 (s, 1H), 8.10 (s, 1H), 3.31 (s, 6H), 3.05 (quint, J = 6.9 Hz, 4H), 2.15 (quint, J = 7.3 Hz, 2H). MS (ESI+): *m/z* 247.0 ((M+H)+).

3-(benzyl(methyl)amino)-7,8-dihydro-6H-indeno[5,6-e][1,2,4]triazine 1,4-dioxide (20t)—Synthesized from **19** using Method F. Red solid. ^{1}H-NMR ($CDCl_3$, 300 MHz): δ 8.24 (s, 1H), 8.16 (s, 1H), 7.25–7.35 (m, 5H), 5.1 (s, 2H), 3.17 (s, 3H), 3.12 (quint, J = 7.6 Hz, 4H), 2.21 (quint, J = 7.6 Hz, 2H). MS (ESI+): *m/z* 323.0 ((M+H)+).

3-(methyl(phenethyl)amino)-7,8-dihydro-6H-indeno[5,6-e][1,2,4]triazine 1,4-dioxide (20u)—Synthesized from **19** using Method F. Red solid. ^{1}H-NMR ($CDCl_3$, 300 MHz): δ 8.09 (s, 1H), 8.05 (s, 1H), 7.21 (d, J = 7.4 Hz, 2H), 7.11 (t, J = 5.2 Hz, 2H), 7.00 (t, J = 7.4 Hz, 1H), 4.16 (t, J = 7.6 Hz, 2H), 3.24 (s, 3H), 2.97–3.11 (m, 6H), 2.18 (quint, J = 7.6 Hz, 2H). MS (ESI+): *m/z* 337.0 ((M+H)+).

3-(thiomorpholinosulfone-1-yl)-7,8-dihydro-6H-indeno[5,6-e][1,2,4]triazine 1,4-dioxide (20v)—Synthesized from **19** using Method F. Red solid. ^{1}H-NMR ($CDCl_3$, 300 MHz): δ 8.17 (s, 1H), 8.14 (s, 1H), 4.35 (m, 2H), 3.26 (m, 2H), 3.12 (m, 2H), 2.23 (quint, J = 7.4 Hz, 2H). MS (ESI+): *m/z* 337.0 ((M+H)+).

3-(2-methylpiperidin-1-yl)-7,8-dihydro-6H-indeno[5,6-e][1,2,4]triazine 1,4-dioxide (20w)—Synthesized from **19** using Method F. Red solid. ^{1}H-NMR ($CDCl_3$, 300 MHz): δ 8.16 (s, 1H), 8.12 (s, 1H), 4.18 (t, J = 7.0 Hz, 1H), 4.18 (d, J = 13.2 Hz, 1H), 3.32 (m, 1H), 3.03 (m, 4H), 2.16 (quint, J = 7.3 Hz, 2H), 1.92 (m, 1H), 1.62 (m, 6H), 1.33 (d, J = 7.0 Hz, 3H). MS (ESI+): *m/z* 301.0 ((M+H)+).

3-(4-(methylsulfonyl)piperazin-1-yl)-7,8-dihydro-6H-indeno[5,6-e][1,2,4]triazine 1,4-dioxide (20x)—Synthesized from **19** using Method F. Red solid. ^{1}H-NMR ($CDCl_3$, 300 MHz): δ 8.15 (s, 1H), 8.12 (s, 1H), 3.95 (m, 4H), 3.42 (m, 4H), 3.07 (quint, J = 5.9 Hz, 4H), 2.79 (s, 3H), 2.17 (quint, J = 7.7 Hz, 2H). MS (ESI+): *m/z* 366.0 ((M+H)+).

Calculation of LUMO Energies

Molecular orbital energy calculations were performed using the semiempirical quantum chemistry program MOPAC2009.[52] The calculation was performed with the Neglect of Diatomic Differential Overlap (NDDO) approximation method with the PM6 parameterization. The geometries of all compounds were optimized using the default Eigenvector Following routine until a self-consistent field was achieved. The energies of the LUMO for each molecule is approximated by the eigenvalues (in eV) of the appropriate orbital generated using the EIGEN and VECTORS keywords.

Bacterial strains, growth conditions, and chemicals

Mtb strains were obtained from the American Type Culture Collection (ATCC, VA) and Colorado State University (CSU) and cultured in roller bottles (Corning Inc) using Middlebrook 7H9 broth (Difco Laboratories) supplemented with 0.2% glycerol, 0.05% Tween-80, and 10% albumin-dextrose-catalase (Difco Laboratories). Middlebrook 7H10 agar (Difco Laboratories), supplemented with 0.2% glycerol and 10% oleic acid-albumin-dextrose-catalase (Difco Laboratories), was used to visualize colonies. Mtb H37Rv was grown in 7H9 broth at 37°C to the mid-log phase. The antibiotics and resazurin were purchased from Sigma (St. Louis, MO) and resuspended according to the manufacturer's instructions. Experiments performed at the Institute for Tuberculosis Research at the University of Illinois Chicago (TB MIC-ITR) were performed according to published methods.[11,53]

Determination of antibiotic susceptibility

To determine the MIC of compounds against Mtb, the resazurin-based microplate assay was performed. Briefly, the compounds were resuspended in DMSO and tested in a range from 10–0.08 mg/L following a two-fold dilution scheme. After addition of the bacterial cells ~10^5 colony forming unit (CFU)/mL, the 96 well plates were incubated at 37°C for 5 d. The addition of 0.05 mL of 0.1% resazurin followed, with additional incubation for 2 d at 37°C. Fluorescence was measured using a Fluoroskan Ascent or Victor 3 microplate fluorimeter (Thermo Scientific, USA) with an excitation of 530nm and emission of 590nm. Wells containing compounds only were used to detect autofluorescence of compounds. The lowest drug concentration that inhibited ≥90% growth was considered to be the MIC. In addition to the fluorescence readouts, all of the MIC values are also scored by visual inspection for confirmation of the MIC value. A two-fold variation in MIC was considered to be within the error range of the assay. The final concentration of DMSO in all wells was 0.625%. These data are presented in Tables 1–5.

Antimicrobial activity against NRP Mtb cells

The antimicrobial activity of various compounds against NRP Mtb cells was determined as described previously using LORA.[7] Briefly, Mtb H37Rv cells were suspended in Middlebrook 7H12 broth and sonicated for 15 s. Cultures were diluted to obtain an OD_{570} of 0.03–0.05 and 3000–7000 relative light units (RLU) per 100 μL. Two-fold serial dilutions of antimicrobial agents were prepared in a volume of 100 μL in black 96-well microtiter plates, and 100 μL of the cell suspension was added. The microplate cultures were placed under anaerobic conditions (O_2 <0.16%) using an Anoxomat Model WS-8080 (MART Microbiology) using three cycles of evacuation and filling with a mixture of 10% H_2, 5% CO_2, and the balance N_2. An anaerobic indicator strip was placed inside the chamber to visually confirm the removal of O_2. Plates are incubated at 37°C for 10 d and then transferred to an ambient gaseous condition (5% CO_2-enriched air) incubator for a 28-h "recovery". On day 11 (after the 28-h aerobic recovery), 100 μL culture were transferred to

white 96-well microtiter plates for determination of luminescence. The MIC was defined as the lowest drug concentration effecting an inhibition of ~90% relative to drug-free controls.

Cytotoxicity Against Vero Cells

The compounds were tested for cytotoxicity against Vero cells using the Cell Titer-Glo Luminescent Cell Viability Assay (Promega). The Vero cells (Vero ATCC CCL-81) were grown and maintained in minimal essential medium (MEM) + 0.25% fetal bovine serum (FBS). Compound dilutions were done in accordance with Clinical and Laboratory Standards Institute (CLSI) guidelines in 96-well plates. Each well contained 5 μL of compound and 95 μL of host Vero cells at a concentration of ~5×10^4 cells/mL. Plates were incubated for 72 h at 37°C + 5% CO_2, followed by equilibration of the plate to room temperature for ~30 min. Addition of the Cell Titer-Glo reagent followed, with mixing the contents for 2 min on an orbital shaker to induce cell lysis and further incubation at room temperature for 10 min to stabilize the luminescent signal. The plates were read and the luminescence was recorded. Each test plate contained a set of controls including media only (for background subtraction) and 0.625% DMSO controls (for calculating the percent viability for all test wells). In addition, each test plate contained an ATP standard curve, which was used to calculate the ATP units in each test well. The toxicity was defined as the concentration at which host cells are 50% viable (IC_{50}).

Mouse lymphoma cell tk+/−→tk−/− gene mutation assay

Experiments were conducted using a standard procedure for evaluating mutagenic potential.[23,24] The details on cell line, experimental procedures and data interpretaion have been previously published.[54] The following endpoints were evaluated in cells following exposure to **15fa** and 20**q**: cell growth during expression periods, relative suspension growth, relative total growth, relative cloning efficiency, mutation frequency, and numbers of small (≤ 0.6 mm in diameter) colonies from trifluorothymidine-resistant (TFT^r) cells.

Solubility Assays

Compounds were ground into a fine powders using a mortar and pestle and added to a 25 mL glass Erlenmeyer flask with 5 mL of a 0.9% saline solution at pH 7.4. Approximately 20 mg of compound was added to each flask to ensure saturation. The flasks were then vigorously stirred using a magnetic stir bar at 25°C for 48 hours. The samples were then filtered through a Whatman PVDF membrane (0.45 μm pore size) syringe filter. The concentration of compound in the supernatant was then measured using HPLC quantitation at the maximum absorption wavelength for each compound. The integration was then fit to a standard curve generated for each compound (R^2 values > 0.99) to determine the equilibrium solubility for each compound.

Pharmacokinetic Studies in Female CD1 Mice

All pharmacokinetic studies were performed in accordance with SRI International's animal care policies in an AAALAC and OLAW accredited facility. The procedure for the pharmacokinetics studies followed a previously described method.[55] Briefly, the plasma pharmacokinetics of selected BTO derivatives were determined in female CD1 mice after administration of a single dose (100 mg/kg) by oral gavage. Blood was collected from three mice per time point at 5, 15, 30, and 60 min and 2, 4, 6, 8, and 24 h after dose administration. Means and standard deviations were calculated for the plasma drug concentrations at each time point. Pharmacokinetic analysis was performed using non compartmental methods (WinNonlin® Professional, Version 5.2, Pharsight Corp, Mountain View, CA). The following parameters were calculated: time to maximum plasma concentration (T_{max}), maximum plasma concentration (C_{max}), maximum plasma

concentration extrapoloated to time 0 (C_0), area under the plasma concentration-time curve to the last time point (AUC_{last}) and to infinity (AUC_{inf}).

Supplementary Material

Refer to Web version on PubMed Central for supplementary material.

Acknowledgments

The project described was supported by Award R56AI090817 from the National Institute of Allergy and Infectious Diseases. The content is the sole responsibility of the authors and does not necessarily represent the official views of the National Institute of Allergy and Infectious Diseases or the National Institutes of Health. Some of the antimicrobial screening was also supported by National Institutes of Health and the National Institute of Allergy and Infectious Diseases, Contract HHSN266200600011C (N01-AI-60011).

Abbreviations used

ATCC	American Type Culture Collection
BTO	1,2,4-benzotriazine di-N-oxides
CC_{50}	cytotoxicity concentration
$CDCl_3$	deuterated chloroform
CD_3OD	deuterated methanol
CFU	colony forming unit
CLSI	Clinical and Laboratory Standards Institute
CSI	Colorado State University
DOTS	direct observed therapy short-course
$E_{½}$	one electron reduction potential
ES-MS	electrospray mass spectra
FBS	fetal bovine serum
LC-MS-MS	liquid chromatograph tandem mass spectrometer
LCQ	liquid chromatography quadrupole
LORA	low-oxygen recovery assay
MDR-TB	multidrug-resistant TB
MEM	minimal essential medium
MLM	mouse liver microsome
MOLY	mouse lymphoma cell mutation assay
Mtb	*Mycobacterium tuberculosis*
NRP	nonreplicating persistence
RLU	relative light unit
SD	standard deviation
SI	selectivity index
TB	tuberculosis
TFAA	trifluoroacetic anhydride

TI	therapeutic index
TPZ	tirapazamine
XDR	extensively drug-resistant

References

1. Gillespie SH. Evolution of drug resistance in Mycobacterium tuberculosis: clinical and molecular perspective. Antimicrob Agents Chemother. 2002; 46:267–274. [PubMed: 11796329]
2. Wayne LG, Hayes LG. An in vitro model for sequential study of shiftdown of Mycobacterium tuberculosis through two stages of nonreplicating persistence. Infect Immun. 1996; 64:2062–2069. [PubMed: 8675308]
3. Stover CK, Warrener P, VanDevanter DR, Sherman DR, Arain TM, Langhorne MH, Anderson SW, Towell JA, Yuan Y, McMurray DN, Kreiswirth BN, Barry CE, Baker WR. A small-molecule nitroimidazopyran drug candidate for the treatment of tuberculosis. Nature. 2000; 405:962–966. [PubMed: 10879539]
4. Matsumoto M, Hashizume H, Tomishige T, Kawasaki M, Tsubouchi H, Sasaki H, Shimokawa Y, Komatsu M. OPC-67683, a nitro-dihydro-imidazooxazole derivative with promising action against tuberculosis in vitro and in mice. PLoS Med. 2006; 3:e466. [PubMed: 17132069]
5. Diacon AH, Dawson R, Hanekom M, Narunsky K, Venter A, Hittel N, Geiter LJ, Wells CD, Paccaly AJ, Donald PR. Early bactericidal activity of delamanid (OPC-67683) in smear-positive pulmonary tuberculosis patients. Int J Tuberc Lung Dis. 2011; 15:949–954. [PubMed: 21682970]
6. Diacon AH, Dawson R, Hanekom M, Narunsky K, Maritz SJ, Venter A, Donald PR, van Niekerk C, Whitney K, Rouse DJ, Laurenzi MW, Ginsberg AM, Spigelman MK. Early bactericidal activity and pharmacokinetics of PA-824 in smear-positive tuberculosis patients. Antimicrob Agents Chemother. 2010; 54:3402–3407. [PubMed: 20498324]
7. Tasneen R, Li SY, Peloquin CA, Taylor D, Williams KN, Andries K, Mdluli KE, Nuermberger EL. Sterilizing Activity of Novel TMC207- and PA-824-Containing Regimens in a Murine Model of Tuberculosis. Antimicrob Agents Chemother. 2011; 55:5485–5492. [PubMed: 21930883]
8. Compounds 1–6 were obtained through the National Institute of Health, National Cancer Institute, Developmental Therapeutics Program. 2003.
9. Dirlam JP, Presslitz JE, Williams BJ. Synthesis and antibacterial activity of some 3-[(alkylthio)methyl]quinoxaline 1-oxide derivatives. J Med Chem. 1983; 26:1122–1126. [PubMed: 6876079]
10. Kelson AB, McNamara JP, Pandey A, Ryan KJ, Dorie MJ, McAfee PA, Menke DR, Brown JM, Tracy M. 1,2,4-Benzotriazine 1,4-dioxides. An important class of hypoxic cytotoxins with antitumor activity. Anticancer Drug Des. 1998; 13:575–592. [PubMed: 9755719]
11. Cho SH, Warit S, Wan B, Hwang CH, Pauli GF, Franzblau SG. Low-oxygen-recovery assay for high-throughput screening of compounds against nonreplicating Mycobacterium tuberculosis. Antimicrob Agents Chemother. 2007; 51:1380–1385. [PubMed: 17210775]
12. Ioerger TR, Feng Y, Ganesula K, Chen X, Dobos KM, Fortune S, Jacobs WR Jr, Mizrahi V, Parish T, Rubin E, Sassetti C, Sacchettini JC. Variation among genome sequences of H37Rv strains of Mycobacterium tuberculosis from multiple laboratories. J Bacteriol. 2010; 192:3645–3653. [PubMed: 20472797]
13. Hay MP, Hicks KO, Pchalek K, Lee HH, Blaser A, Pruijn FB, Anderson RF, Shinde SS, Wilson WR, Denny WA. Tricyclic [1,2,4]triazine 1,4-dioxides as hypoxia selective cytotoxins. J Med Chem. 2008; 51:6853–6865. [PubMed: 18847185]
14. Perola E. An Analysis of the Binding Efficiencies of Drugs and Their Leads in Successful Drug Discovery Programs. Journal of Medicinal Chemistry. 2010; 53:2986–2997. [PubMed: 20235539]
15. Boshoff HI, Barry CE 3rd. Tuberculosis - metabolism and respiration in the absence of growth. Nat Rev Microbiol. 2005; 3:70–80. [PubMed: 15608701]
16. Carmeli M, Rozen S. A new efficient route for the formation of quinoxaline N-oxides and N,N′-dioxides using HOF. CH3CN. J Org Chem. 2006; 71:5761–5765. [PubMed: 16839160]

17. Carmeli M, Rozen S. Oxidation of azides by the HOF. CH3CN: a novel synthesis of nitro compounds. J Org Chem. 2006; 71:4585–4589. [PubMed: 16749792]

18. Medjahed H, Gaillard JL, Reyrat JM. Mycobacterium abscessus: a new player in the mycobacterial field. Trends in Microbiology. 2010; 18:117–123. [PubMed: 20060723]

19. Olive PL, Banath JP, Durand RE. Detection of subpopulations resistant to DNA-damaging agents in spheroids and murine tumours. Mutat Res. 1997; 375:157–165. [PubMed: 9202726]

20. Voogd CE. On the mutagenicity of nitroimidazoles. Mutat Res. 1981; 86:243–277. [PubMed: 6457989]

21. Ames BN, McCann J, Yamasaki E. Methods for detecting carcinogens and mutagens with the Salmonella/mammalian-microsome mutagenicity test. Mutat Res. 1975; 31:347–364. [PubMed: 768755]

22. McCann J, Spingarn NE, Kobori J, Ames BN. Detection of carcinogens as mutagens: bacterial tester strains with R factor plasmids. Proc Natl Acad Sci U S A. 1975; 72:979–983. [PubMed: 165497]

23. Clive D, Johnson KO, Spector JF, Batson AG, Brown MM. Validation and characterization of the L5178Y/TK+/− mouse lymphoma mutagen assay system. Mutat Res. 1979; 59:61–108. [PubMed: 372791]

24. Moore MM, Honma M, Clements J, Harrington-Brock K, Awogi T, Bolcsfoldi G, Cifone M, Collard D, Fellows M, Flanders K, Gollapudi B, Jenkinson P, Kirby P, Kirchner S, Kraycer J, McEnaney S, Muster W, Myhr B, O'Donovan M, Oliver J, Ouldelhkim MC, Pant K, Preston R, Riach C, San R, Shimada H, Stankowski LF Jr. Mouse lymphoma thymidine kinase gene mutation assay: follow-up International Workshop on Genotoxicity Test Procedures, New Orleans, Louisiana, April 2000. Environ Mol Mutagen. 2002; 40:292–299. [PubMed: 12489120]

25. Koul A, Arnoult E, Lounis N, Guillemont J, Andries K. The challenge of new drug discovery for tuberculosis. Nature. 2011; 469:483–490. [PubMed: 21270886]

26. Cherian J, Choi I, Nayyar A, Manjunatha UH, Mukherjee T, Lee YS, Boshoff HI, Singh R, Ha YH, Goodwin M, Lakshminarayana SB, Niyomrattanakit P, Jiricek J, Ravindran S, Dick T, Keller TH, Dartois V, Barry CE 3rd. Structure-activity relationships of antitubercular nitroimidazoles. 3. Exploration of the linker and lipophilic tail of ((s)-2-nitro-6, 7-dihydro-5H-imidazo[2, 1-b][1, 3]oxazin-6-yl)-(4-trifluoromethoxybenzyl)amine (6-amino PA-824). J Med Chem. 2011; 54:5639–5659. [PubMed: 21755942]

27. Kim P, Kang S, Boshoff HI, Jiricek J, Collins M, Singh R, Manjunatha UH, Niyomrattanakit P, Zhang L, Goodwin M, Dick T, Keller TH, Dowd CS, Barry CE 3rd. Structure-activity relationships of antitubercular nitroimidazoles. 2. Determinants of aerobic activity and quantitative structure-activity relationships. J Med Chem. 2009; 52:1329–1344. [PubMed: 19209893]

28. Kim P, Zhang L, Manjunatha UH, Singh R, Patel S, Jiricek J, Keller TH, Boshoff HI, Barry CE 3rd, Dowd CS. Structure-activity relationships of antitubercular nitroimidazoles. 1. Structural features associated with aerobic and anaerobic activities of 4- and 5-nitroimidazoles. J Med Chem. 2009; 52:1317–1328. [PubMed: 19209889]

29. Palmer BD, Thompson AM, Sutherland HS, Blaser A, Kmentova I, Franzblau SG, Wan B, Wang Y, Ma Z, Denny WA. Synthesis and structure-activity studies of biphenyl analogues of the tuberculosis drug (6S)-2-nitro-6-{[4-(trifluoromethoxy)benzyl]oxy}-6,7-dihydro-5H-imidazo[2,1-b][1, 3]oxazine (PA-824). J Med Chem. 2010; 53:282–294. [PubMed: 19928920]

30. Thompson AM, Blaser A, Anderson RF, Shinde SS, Franzblau SG, Ma Z, Denny WA, Palmer BD. Synthesis, reduction potentials, and antitubercular activity of ring A/B analogues of the bioreductive drug (6S)-2-nitro-6-{[4-(trifluoromethoxy)benzyl]oxy}-6,7-dihydro-5H-imidazo[2,1-b][1, 3]oxazine (PA-824). J Med Chem. 2009; 52:637–645. [PubMed: 19099398]

31. Hodgkiss RJ. Use of 2-nitroimidazoles as bioreductive markers for tumour hypoxia. Anticancer Drug Des. 1998; 13:687–702. [PubMed: 9755725]

32. Hevener KE, Ball DM, Buolamwini JK, Lee RE. Quantitative structure-activity relationship studies on nitrofuranyl anti-tubercular agents. Bioorg Med Chem. 2008; 16:8042–8053. [PubMed: 18701298]

33. Tangallapally RP, Yendapally R, Lee RE, Lenaerts AJ. Synthesis and evaluation of cyclic secondary amine substituted phenyl and benzyl nitrofuranyl amides as novel antituberculosis agents. J Med Chem. 2005; 48:8261–8269. [PubMed: 16366608]
34. Ancizu S, Moreno E, Solano B, Villar R, Burguete A, Torres E, Perez-Silanes S, Aldana I, Monge A. New 3-methylquinoxaline-2-carboxamide 1,4-di-N-oxide derivatives as anti-Mycobacterium tuberculosis agents. Bioorg Med Chem. 2010; 18:2713–2719. [PubMed: 20233660]
35. Moreno E, Ancizu S, Perez-Silanes S, Torres E, Aldana I, Monge A. Synthesis and antimycobacterial activity of new quinoxaline-2-carboxamide 1,4-di-N-oxide derivatives. Eur J Med Chem. 2010; 45:4418–4426. [PubMed: 20656380]
36. Ortega MA, Sainz Y, Montoya ME, Lopez De Cerain A, Monge A. Synthesis and antituberculosis activity of new 2-quinoxalinecarbonitrile 1,4-di-N-oxides. Pharmazie. 1999; 54:24–25. [PubMed: 9987794]
37. Torres E, Moreno E, Ancizu S, Barea C, Galiano S, Aldana I, Monge A, Perez-Silanes S. New 1,4-di-N-oxide-quinoxaline-2-ylmethylene isonicotinic acid hydrazide derivatives as anti-Mycobacterium tuberculosis agents. Bioorg Med Chem Lett. 2011; 21:3699–3703. [PubMed: 21570839]
38. Vicente E, Perez-Silanes S, Lima LM, Ancizu S, Burguete A, Solano B, Villar R, Aldana I, Monge A. Selective activity against Mycobacteriumtuberculosis of new quinoxaline 1,4-di-N-oxides. Bioorg Med Chem. 2009; 17:385–389. [PubMed: 19058970]
39. Villar R, Vicente E, Solano B, Perez-Silanes S, Aldana I, Maddry JA, Lenaerts AJ, Franzblau SG, Cho SH, Monge A, Goldman RC. In vitro and in vivo antimycobacterial activities of ketone and amide derivatives of quinoxaline 1,4-di-N-oxide. J Antimicrob Chemother. 2008; 62:547–554. [PubMed: 18502817]
40. Vicente E, Villar R, Perez-Silanes S, Aldana I, Goldman RC, Monge A. Quinoxaline 1,4-di-N-oxide and the potential for treating tuberculosis. Infect Disord Drug Targets. 2011; 11:196–204. [PubMed: 21470099]
41. Zeman EM, Baker MA, Lemmon MJ, Pearson CI, Adams JA, Brown JM, Lee WW, Tracy M. Structure-activity relationships for benzotriazine di-N-oxides. Int J Radiat Oncol Biol Phys. 1989; 16:977–981. [PubMed: 2703405]
42. Zeman EM, Brown JM, Lemmon MJ, Hirst VK, Lee WW. SR-4233: a new bioreductive agent with high selective toxicity for hypoxic mammalian cells. Int J Radiat Oncol Biol Phys. 1986; 12:1239–1242. [PubMed: 3744945]
43. Brown JM. Tumor hypoxia, drug resistance, and metastases. J Natl Cancer Inst. 1990; 82:338–339. [PubMed: 2406450]
44. Brown JM. The hypoxic cell: a target for selective cancer therapy--eighteenth Bruce F. Cain Memorial Award lecture. Cancer Res. 1999; 59:5863–5870. [PubMed: 10606224]
45. Delahoussaye YM, Evans JW, Brown JM. Metabolism of tirapazamine by multiple reductases in the nucleus. Biochem Pharmacol. 2001; 62:1201–1209. [PubMed: 11705453]
46. Fitzsimmons SA, Lewis AD, Riley RJ, Workman P. Reduction of 3-amino-1,2,4-benzotriazine-1,4-di-N-oxide (tirapazamine, WIN 59075, SR 4233) to a DNA-damaging species: a direct role for NADPH:cytochrome P450 oxidoreductase. Carcinogenesis. 1994; 15:1503–1510. [PubMed: 8055626]
47. Riley RJ, Hemingway SA, Graham MA, Workman P. Initial characterization of the major mouse cytochrome P450 enzymes involved in the reductive metabolism of the hypoxic cytotoxin 3-amino-1,2,4-benzotriazine-1,4-di-N-oxide (tirapazamine, SR 4233, WIN 59075). Biochem Pharmacol. 1993; 45:1065–1077. [PubMed: 8461036]
48. Wang J, Biedermann KA, Wolf CR, Brown JM. Metabolism of the bioreductive cytotoxin SR 4233 by tumour cells: enzymatic studies. Br J Cancer. 1993; 67:321–325. [PubMed: 8431360]
49. Anderson RF, Shinde SS, Hay MP, Gamage SA, Denny WA. Activation of 3-amino-1,2,4-benzotriazine 1,4-dioxide antitumor agents to oxidizing species following their one-electron reduction. J Am Chem Soc. 2003; 125:748–756. [PubMed: 12526674]
50. Maccoll A. Reduction Potentials of Conjugated Systems. Nature. 1949; 163:178–179.
51. Purwantini E, Gillis TP, Daniels L. Presence of F420-dependent glucose-6-phosphate dehydrogenase in Mycobacterium and Nocardia species, but absence from Streptomyces and

Corynebacterium species and methanogenic Archaea. FEMS Microbiol Lett. 1997; 146:129–134. [PubMed: 8997717]

52. Stewart, JJP. MOPAC2009. Stewart Computational Chemistry; Colorado Springs, CO, USA: 2008.
53. Collins L, Franzblau SG. Microplate alamar blue assay versus BACTEC 460 system for high-throughput screening of compounds against Mycobacterium tuberculosis and Mycobacterium avium. Antimicrob Agents Chemother. 1997; 41:1004–1009. [PubMed: 9145860]
54. Doppalapudi RS, Riccio ES, Rausch LL, Shimon JA, Lee PS, Mortelmans KE, Kapetanovic IM, Crowell JA, Mirsalis JC. Evaluation of chemopreventive agents for genotoxic activity. Mutat Res. 2007; 629:148–160. [PubMed: 17387038]
55. Ray S, Madrid PB, Catz P, LeValley SE, Furniss MJ, Rausch LL, Guy RK, DeRisi JL, Iyer LV, Green CE, Mirsalis JC. Development of a new generation of 4-aminoquinoline antimalarial compounds using predictive pharmacokinetic and toxicology models. J Med Chem. 2010; 53:3685–3695. [PubMed: 20361799]

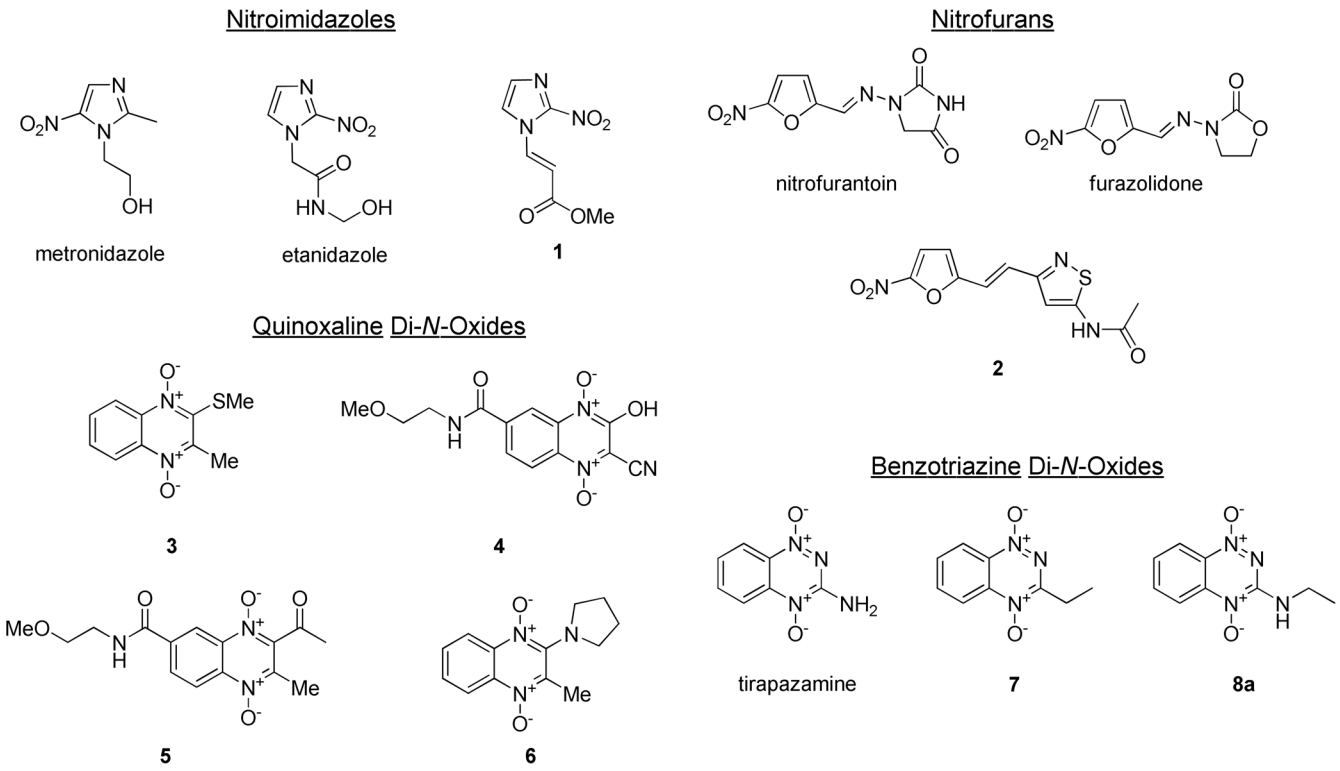

Figure 1.

A) Chemical structures of bioreductively-activated compounds with known antimicrobial activities.

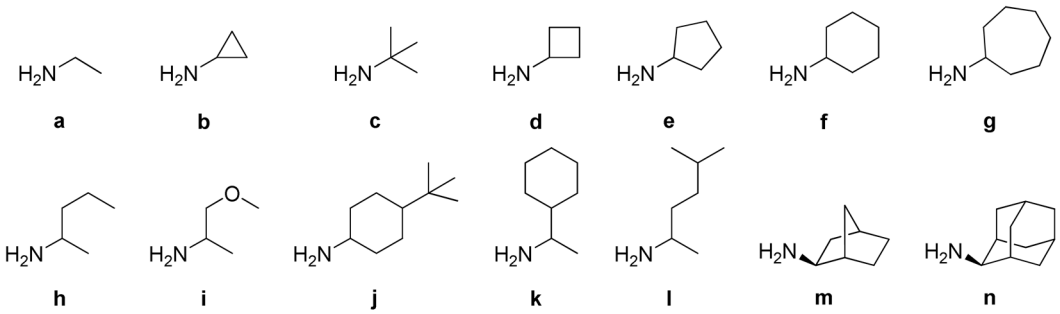

Figure 2.
Amine diversity elements used for side chains on benzotriazines.

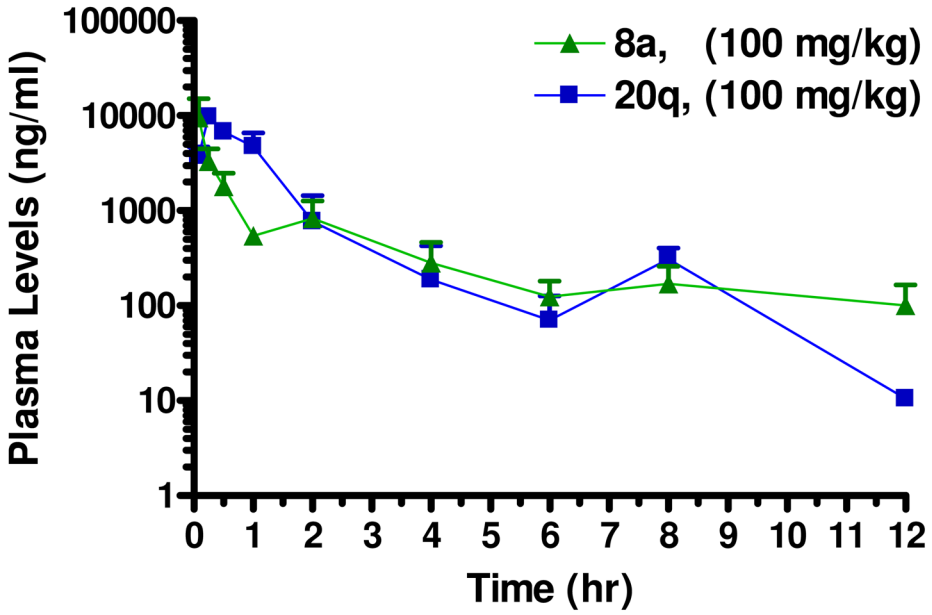

Figure 3.

Plasma drug concentrations of **8a** and **20q** in female Balb/c mice (n = 3 mice per time point) after po administration of 100 mg/kg of each compound. Blood was collected at time points through 24 hr post-dose, processed to plasma and analyzed for each of the test compounds. The concentrations at the 24 hr time point for both compounds was lower than the limit of quantitation.

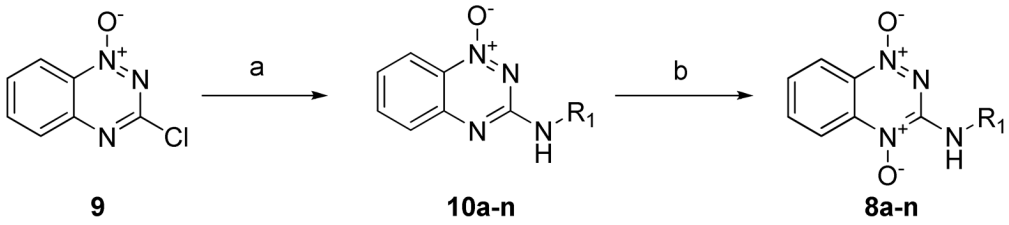

Scheme 1.

Synthesis of *N*-alkyl 1,2,4-benzotriazine-di-*N*-oxides. *Reagents and conditions:* (a) RNH_2 (2 eq.), TEA (2 eq.), DCM, 18 h, rt. (b) TFAA, H_2O_2, THF, 4 d.

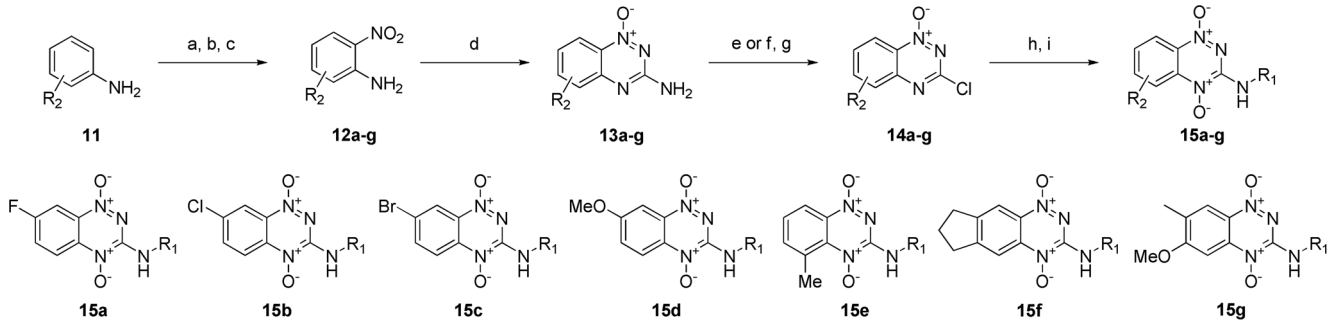

Scheme 2.

Synthesis of ring substituted 1,2,4-benzotriazine-di-*N*-oxides. *Reagents and conditions:* (a) Ac_2O, TEA, DCM. (b) $fHNO_3$, Ac_2O, DCM. (c) HCl, reflux. (d) $NCNH_2$, conc. HCl. (e) $NaNO_2$, HCl. (f) tBuONO, tBuOH, H_2O. (g) $POCl_3$, reflux. (h) RNH_2 (2 eq.), TEA (2 eq.), DCM, 18 h, rt. (i) TFAA, H_2O_2, THF, 4 d.

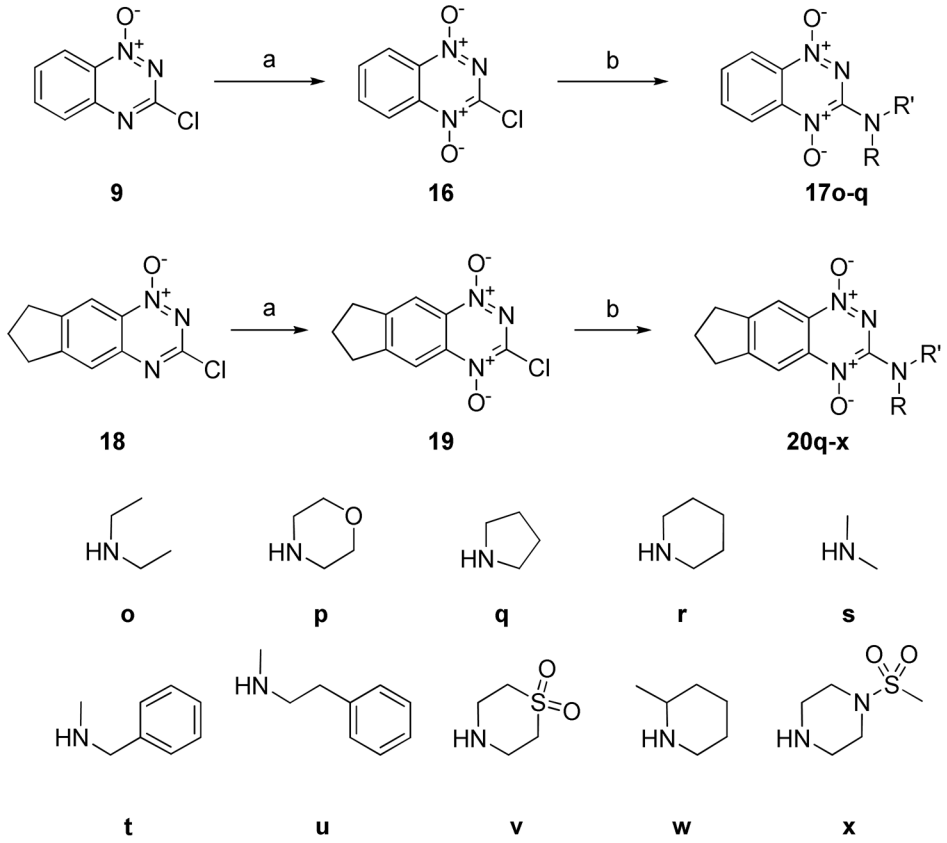

Scheme 3.

Synthesis of di-*N*-alkyl 1,2,4-benzotriazine-di-*N*-oxides. *Reagents and conditions:* (a) F_2 (g), H_2O, MeCN (b) RNH_2 (2 eq.), TEA (2 eq.), DCM, 1 h, rt.

Table 1

Antitubercular activity of different scaffolds of bioreductively-activated antimicrobial compounds.

Classification	Compound	LUMO (eV)	TB MIC – SRI (μg/mL)	TB MIC –ITR (μg/mL)	LORA MIC – ITR (μg/mL)	Vero Tox CC_{50} (μg/mL)	SI (CC_{50}/MIC)
Isoniazid	INH	–	0.060	0.091	>20	>50	>830
Rifampin	RIF	–	0.003	0.041	2.0	>50	>15000
Nitroimidazole	Metronidazole	−1.303	>10	>32	11	>16	NA
	Etanidazole	−1.644	>10	>32	26	>16	NA
	1	−1.802	10	29	3.3	16	1.6
Nitrofurans	Nitrofurantoin	−1.801[a]	16	28	32	23	1.1
	Furazolidone	−1.652[a]	31	30	6.5	19	0.60
	2	−1.660[a]	0.98	3.8	3.7	>50	>50
Quinoxaline-1,4-di-*N*-oxides	**3**	−1.452	10	28	9.4	>16	>1.6
	4	−2.436	>20	>32	>32	>16	NA
	5	−1.919	10	27	>32	>16	>1.6
	6	−1.279	>10	>32	>32	>16	NA
Benzotriazine-1,4-di-*N*-oxides	TPZ	−1.622	5.0	3.7	7.3	8.0	1.6
	7	−1.703	5.0	3.7	0.97	38	7.6
	8a	−1.442	1.2	0.57	0.37	17	17

[a]Calculation performed for Z stereochemistry around double bond.

NA = not available; ITR = Institute for Tuberculosis Research, University of Illinois at Chicago.

J Med Chem. Author manuscript; available in PMC 2013 July 12.

Table 2

Antitubercular activity of side-chain-substituted BTOs.

Compound	LUMO (eV)	TB MIC – SRI (μg/mL)	TB MIC – ITR (μg/mL)	LORA MIC – ITR (μg/mL)	Vero Tox CC_{50} (μg/mL)	SI (CC_{50}/MIC)
8b	−1.652	2.5	1.8	1.8	21	8.3
8c	−1.414	1.2	1.9	0.82	8.0	6.4
8d	−1.589	1.2	0.94	0.84	8.9	7.1
8e	−1.555	2.5	3.6	0.68	10	4.2
8f	−1.536	2.5	3.8	0.75	8.9	3.6
8g	−1.514	2.5	1.6	0.50	7.9	3.2
8h	−1.530	5.0	1.9	0.99	26	5.3
8i	−1.412	10.0	6.6	4.9	>50	>5.0
8j	−1.523	0.62	0.22	<0.12	2.3	3.7
8k	−1.495	1.2	0.92	0.36	8.9	7.1
8l	−1.532	1.2	0.52	0.38	4.1	3.3
8m	−1.553	0.62	0.60	0.42	3.4	5.5
8n	−1.501	2.5	1.9	2.3	7.3	2.9

J Med Chem. Author manuscript; available in PMC 2013 July 12.

Table 3

Antitubercular activity of ring-substituted BTOs.

Compound	LUMO (eV)	TB MIC – SRI (μg/mL)	TB MIC – ITR (μg/mL)	LORA MIC – ITR (μg/mL)	Vero Tox CC_{50} (μg/mL)	SI (CC_{50}/MIC)
15aa	−1.704	0.62	0.35	0.75	4.6	7.3
15ab	−1.918	0.31	0.93	3.5	1.3	2.2
15ad	−1.857	0.31	0.40	0.88	1.6	10
15ae	−1.820	0.31	0.33	0.34	2.3	7.3
15af	−1.696	0.62	0.68	0.47	<2.5	<4.0
15ai	−1.716	5.0	2.0	1.9	6.3	1.3
15am	−1.808	0.31	<0.12	0.21	<2.5	<4.0
15ba	−1.666	1.2	<0.12	0.41	2.6	2.1
15bb	−1.870	0.62	0.21	0.22	1.3	2.2
15bd	−1.812	0.15	<0.12	<0.12	1.6	10
15bf	−1.655	0.62	0.94	0.63	2.6	4.2
15bi	−1.675	1.2	1.4	0.78	2.6	2.1
15bm	−1.759	0.15	0.22	0.23	1.1	7.3
15ca	−1.652	0.62	0.49	0.46	4.2	6.7
15cd	−1.793	0.15	0.46	0.41	3.8	24
15ce	−1.757	0.15	0.35	0.46	18	110
15cm	−1.749	0.31	0.36	0.41	0.80	2.6
15da	−1.541	2.5	15	16	16	6.3
15dd	−1.66	0.62	0.96	0.90	9.8	16
15dm	−1.629	0.62	0.97	1.6	>50	>80
15ea	−1.409	0.62	0.51	0.48	22	36
15ed	−1.567	0.31	0.47	0.43	22	70
15ee	−1.524	0.31	0.43	0.27	3.7	12
15fa	−1.254	1.2	0.95	0.83	36	29
15fd	−1.352	0.62	0.96	0.44	34	54
15fm	−1.244	1.2	0.93	0.36	>50	>41
15ga	−1.195	2.5	3.5	2.5	>100	>40

J Med Chem. Author manuscript; available in PMC 2013 July 12.

Compound	LUMO (eV)	TB MIC – SRI (μg/mL)	TB MIC – ITR (μg/mL)	LORA MIC – ITR (μg/mL)	Vero Tox CC_{50} (μg/mL)	SI (CC_{50}/MIC)
15gd	−1.324	2.5	5.1	2.9	>50	>20
15gm	−1.284	5.0	5.6	3.5	>50	>10

Table 4

Antitubercular activity of di-*N*-alkyl BTOs.

Compound	LUMO (eV)	TB MIC – SRI (μg/mL)	TB MIC – ITR (μg/mL)	LORA MIC – ITR (μg/mL)	Vero Tox CC_{50} (μg/mL)	SI (CC_{50}/MIC)
17o	−1.483	0.31	0.46	1.3	12	40
17p	−1.624	2.5	3.7	19	5.4	2.2
17q	−1.286	0.31	NT	NT	17	56
20q	−1.196	0.31	0.46	0.99	25	80
20r	−1.311	0.62	0.40	0.49	21	13
20s	−1.335	0.62	0.30	1.5	24	13
20t	−1.344	0.31	0.15	0.41	17	53
20u	−1.289	0.31	0.24	0.44	40	130
20v	−1.751	5.0	15	30	17	3.4
20w	−1.293	1.2	0.66	0.47	>50	>40
20x	−1.258	5.0	13	15	>50	>10

J Med Chem. Author manuscript; available in PMC 2013 July 12.

Table 5

MIC of BTO's against Single Drug Resistant Mtb strains.

		MIC Values (μg/mL) of Mtb Strains Resistant to:					
Compound	**H37Rv**	**Strepto-mycin ATCC 35820**	**P-amino-salicyclic acid ATCC 35821**	**Isoniazid ATCC 35822**	**Kanamycin ATCC 35827**	**Ethionami de ATCC 35830**	**Etham-butol ATCC 35837**
8a	1.2	1.2	1.2	1.2	1.2	1.2	1.2
8c	2.5	1.2	1.2	2.5	2.5	1.2	2.5
15ea	0.62	0.16	0.31	0.62	0.62	0.31	0.62
15fa	1.2	0.63	1.2	2.5	1.2	1.2	1.2
15fd	0.62	0.31	0.62	1.2	1.2	0.62	0.62
15ga	1.2	1.2	1.2	1.2	1.2	1.2	1.2
17q	0.31	0.02	0.62	0.31	0.31	0.31	0.31
20q	0.62	0.16	0.31	0.31	0.63	0.62	0.62
20r	0.62	0.15	0.31	0.15	0.31	0.31	0.31
20s	0.62	<0.07	0.15	<0.07	0.31	0.15	0.31
20t	0.31	<0.07	0.07	<0.07	0.15	0.07	0.15
20u	0.31	<0.07	0.15	0.07	0.15	0.15	0.31
20w	1.2	0.31	0.62	0.31	0.62	0.31	0.62

J Med Chem. Author manuscript; available in PMC 2013 July 12.

Table 6

Mutagenic potential of BTOs in MOLY assay. (S9 = Rat metabolic activation; Positive = A significant induction of mutation frequency; Negative = No significant induction of mutation frequency; NT = Not tested)

Compound	Dose (μg/mL)	−S9, 4-Hr Exposure	−S9, 24-Hr Exposure	+S9, 4-Hr Exposure	+S9, 24-Hr Exposure
15fa	10	Positive	NA	Positive	Positive
	25	Positive	NA	Positive	Positive
	50	Positive	NA	Positive	Positive
	100	Positive	NA	Positive	Positive
20q	10	Negative	Negative	Negative	Negative
	25	Negative	Negative	Negative[a]	Negative
	50[a]	Negative	Negative	Negative	Negative
	100 [a]	Negative	Negative	Negative	Negative

[a]Induction of mutation frequency but slightly higher than 40×10^{-6} net over mean solvent control, biologically considered negative.

Table 7

Pharmacokinetic Parameters for **8a** and **20q** after Oral Administration to Female Mice.

Compound	Dose (mg/kg)	$t_{1/2}$ (hr)	T_{max} (hr)	C_{max} (ng/ml)	AUC_{last} (hr·ng/ml)	AUC_{inf} (hr·ng/ml)
8a	100	1.5	0.08	9540	6578	6937
20q	100	1.9	0.25	9767	11219	11248